2014•2015
FACULTEIT GENEESKUNDE EN LEVENSWETENSCHAPPEN
*master in de biomedische wetenschappen*

# Masterproef

## Assessing actin-cMyBP-C interactions in IPS cell-derived cardiomyocytes

Promotor :
dr. Annelies BRONCKAERS

Promotor :
Prof.dr. ANGEL RAYA


Jonathan De Smedt
*Scriptie ingediend tot het behalen van de graad van master in de biomedische wetenschappen*

2014•2015
FACULTEIT GENEESKUNDE EN LEVENSWETENSCHAPPEN
*master in de biomedische wetenschappen*

# Masterproef

## Assessing actin-cMyBP-C interactions in IPS cell-derived cardiomyocytes

Promotor :
dr. Annelies BRONCKAERS

Promotor :
Prof.dr. ANGEL RAYA

Jonathan De Smedt

*Scriptie ingediend tot het behalen van de graad van master in de biomedische wetenschappen*

universiteit hasselt | Maastricht University

# Preface

In the context of my Master's senior practical training and dissertation, I chose to put my interest and efforts in the research of familial hypertrophic cardiomyopathy. Cardiovascular diseases are one of the global leading causes of death and hypertrophic cardiomyopathy is the most commonly occurring inheritable cardiovascular disease. Although several mutations have been identified as causes for this disease, the exact mechanisms still remain unclear. In this practical training and dissertation, I will focus on the design of fusion protein constructs in order to investigate the function of one of the proteins involved in hypertrophic cardiomyopathy, more specifically cMyBP-C. Since not much is known yet about this protein's function in both healthy as diseased hearts, there is still a significant amount of research needed in order to reveal the protein's working mechanisms. As this project and this dissertation could not be realised without the help and support of many people, I would like to thank in the first place the Control of Stem Cell Potency laboratory of prof.dr. A. Raya of the Institute for Bioengineering of Catalonia (Barcelona, Spain) for the opportunity to have this project and for the general support. More specifically, I would like to thank my tutor Mr. J.L. Vazquez-Renteria for his daily guidance, support and research discussions and my promotor, prof.dr. A. Raya for his support, coordination of the project and his advice. Furthermore, I would like to thank Y. Richaud-Patin as she was always available and helpful with many practical questions and taught me how to reprogram iPS cells. I would like to thank S. Jimenez-Delgado and C. Calatayud for their explanations and work in the design of the constructs. I also would like to thank my promotor, dr. A. Bronckaers from Hasselt University, who evaluated the work from a distance and to whom I always could come for questions or advice. Lastly, I also would like to thank my family and the people closest to me for their support when I needed it.

# Table of Contents

# List of abbreviations

| | |
|---|---|
| AP | alkaline phosphatase |
| bFGF | basic fibroblast growth factor |
| Cas9 | CRISPR-associated protein 9 |
| CIU | cell infectious units |
| cMyBP-C | cardiac myosin binding protein C |
| CRISPR | Clustered Regularly Interspaced Short Palindromic Repeats |
| DAPI | 4',6-diamidino-2-phenylindole |
| DMSO | dimethylsulfoxide |
| DNA | deoxyribonucleic acid |
| DSB | double-strand break |
| dCTFM | dynamic cell traction force microscopy |
| EB | embryoid body |
| EDTA | ethylenediaminetetraacetic acid |
| EGF | epidermal growth factor |
| ES cell | embryonic stem cell |
| FACS | fluorescence-activated cell sorting |
| FBS | foetal bovine serum |
| FAK | focal adhesion kinase |
| FRET | (Förster) Fluorescence Resonance Energy Transfer |
| GFP | green fluorescent protein |
| GiWi protocol | Gsk3 inhibitor and Wnt inhibitor protocol |
| gRNA | guide ribonucleic acid |
| HCM | familial hypertrophic cardiomyopathy |
| HDF medium | human dermal fibroblast medium |
| HDR | homology-directed repair |
| hES | human embryonic stem cell |
| hES-CM | conditioned human embryonic stem cell medium |
| HF | High Fidelity |
| HFF | human foreskin fibroblast |
| IMDM | Iscove's Modified Dulbecco's Medium |
| iPS cell | induced pluripotent stem cell |
| irr | irradiated |
| IWP-4 | inhibitor of Wnt production 4 |
| KO-DMEM | knock-out Dulbecco's Modified Eagle's Medium |
| KOSR | knock-out serum replacement |
| LIF | leukaemia inhibitory factor |
| MCS | multiple cloning site |
| MEF | mouse embryonic fibroblast |
| MI | myocardial infarct |
| MOI | multiplicity of infection |
| *MYBPC3* | Myosin Binding Protein C 3 gene |
| NEAA | non-essential amino acids |
| NEB | New England Biolabs |
| NHEJ | non-homologous end joining |
| PAM | protospacer-adjacent motif |
| PCR | polymerase chain reaction |
| PEI | polyethylenimine |
| PFA | paraformaldehyde |
| RFP | red fluorescent protein |
| RNA | ribonucleic acid |
| ROCK | Rho-associated protein kinase |
| RPMI | (medium developed at) Roswell Park Memorial Institute |
| RT-PCR | reverse transcriptase polymerase chain reaction |
| SCID | severe combined immunodeficiency |
| SeV | Sendai virus |
| SMA | smooth muscle actin |
| TBS | Tris-buffered saline |
| WT | wild-type |

# Abstract

**Background**

*MYBPC3* mutations have been shown to cause familial hypertrophic cardiomyopathy (HCM). *MYBPC3* codes for cardiac myosin binding protein C (cMyBP-C). It is known that cMyBP-C interacts with myosin and has multiple binding sites for actin. It has been postulated that cMyBP-C plays a crucial role in the actomyosin cross-bridge cycling. Importantly, *MYBPC3* mutations are not fully penetrant, i.e. carriers of a *MYBPC3* mutation may or may not present with HCM symptoms, indicating other factors are involved. As the exact interactions between cMyBP-C and actin are still unknown, we aim in this research to develop new tools for the study of these interactions in disease-specific cells from HCM patients. We focus on the development of fusion proteins to make future Förster Resonance Energy Transfer (FRET) experiments possible. Secondly, we aim to develop a functional reporter fusion gene for cardiomyocytes using CRISPR-Cas9 technology.

**Methods**

Fusion protein constructs for actin and cMyBP-C were designed. *ACTC1* was fused with RFP and *MYBPC3* was fused with GFP. Fusions were made both C-terminally and N-terminally. *ACTC1* constructs were tested in 293T cells to show the proper translation of the fusion genes. *MYBPC3* constructs were tested before in HEK293 cells. Selection was applied in these cell lines to test the functionality of the antibiotic resistance cassette included in the constructs. Both wild-type and HCM patient-derived fibroblasts were reprogrammed to iPS cells. Subsequently, wild-type iPS cells were characterised and transfected with the constructs in all possible *MYBPC3*-*ACTC1* combinations, both in a serial and in a parallel manner, resulting in a total of eight test groups. Afterwards, these iPS cells were selected and differentiated into cardiomyocytes.
In a parallel experiment, an *Nkx2.5*-RFP construct and suitable gRNA sequences were designed in order to integrate an RFP sequence in iPS cells, downstream and adjacent to the *Nkx2.5* gene using CRISPR-Cas9 technology.

**Results**

We show the characterisation of the SP11.1 iPS cell line including the karyotype, DNA methylation, RT-PCR, pluripotency marker staining, *in vitro* differentiation, teratoma formation and alkaline phosphatase staining. HCM patient-derived fibroblasts were successfully reprogrammed into iPS cells by means of Sendai viruses. Maps were designed for the four protein constructs. The fluorescence and thus functionality of the four protein constructs was visualised for three construct concentrations and at three time points after start of selection. The optimal construct concentrations to transfect the respective cell types were determined, after which cells are to be expanded and stored. Additionally, we show an effective differentiation of iPS cells into beating cardiomyocytes.

**Conclusion**

Together, the results provide a basis for future planned experiments such as FRET, dynamic cell traction force microscopy, imaging and comparing of wild-type and HCM-patient derived cardiomyocytes. Additionally, CRISPR-Cas9 mediated construct genomic integration will be designed based on the results of this research.

# 1. Introduction

## 1.1 Familial hypertrophic cardiomyopathy

Familial hypertrophic cardiomyopathy (HCM) is the most common of all genetic cardiovascular diseases and displays an autosomal dominant inheritance pattern. HCM has a prevalence in adults of approximately 0.2% [1] and a mortality rate of 1% in the general HCM patient population. However, mortality rates of up to 11% have been reported in the end-stage HCM patient subpopulation [2]. HCM is characterised by hypertrophia in the left ventricle of the heart **(Supplemental figure S1)**, predominantly in the ventricular septum. HCM is also marked by diastolic dysfunction and a decreased preload, due to decreased compliance and left ventricular volume. Systolic dysfunction typically occurs in end-stage HCM, in which the myocardium thins and the left ventricle enlarges.

HCM causing mutations in ten different genes have been identified, of which ß-myosin heavy chain, cardiac troponin T and cardiac myosin binding protein C are the most common ones [1]. The focus in this project will be on cardiac myosin binding protein C (cMyBP-C), encoded by the *MYPBC3* gene. cMyBP-C is a member of the MYBP family that is expressed solely in cardiac muscle. Other members of this family are the slow-type MyBP-C and fast-type MyBP-C isoforms which have an expression restricted to slow twitch and fast twitch skeletal muscle respectively. Each of these paralogous isoforms are encoded in a different chromosome and hence do not result from alternative splicing but rather from duplication in the course of evolution. cMyBP-C consists of eight immunoglobulin domains, three fibronectin type III domains, a M-domain containing multiple phosphorylations sites and a N-terminal proline-alanine (P/A)-rich region **(Supplemental figure S2)**. cMyBP-C differs from both skeletal muscle isoforms in the presence of an N-terminal C0 immunoglobulin domain, the phosphorylation sites in the M-domain and 28 extra amino acid residues in the C5 immunoglobulin domain [3]. To date, 197 different mutations in cMyBP-C have been identified **(Supplemental figure S3)** [4]. These mutations can be relatively harmless in case of single amino acid mutations. However, mutations in the phosphorylation sites in the M-domain as well as truncating mutations or frameshift mutations could have an impact on the function of the protein.

There is still little known about the exact mechanisms or pathways in which cMyBP-C regulates cardiac muscle contraction. cMyBP-C has binding sites for myosin, actin and titin. However, the exact position, orientation and alignment remain uncertain and have been the subject of several hypotheses, such as the trimeric collar model [5] and the rod model of axial oriented arrangement [6]**(Supplemental figure S4)**. It has been shown that functional cMyBP-C expression is not a necessary requirement for cardiac development or contraction, but the protein rather plays an essential role in the regulation of cardiac muscle contraction [3,7]. More specifically, cMyBP-C provides an essential mechanical constraint on the actomyosin cross-bridge cycling. This constraint might be imposed by constriction of the collar-like arrangement of the C-terminal ends [5,8] as well as by interaction of the N-terminal ends with the myosin heads and actin [4] **(Figure 1)**. As this protein imposes a constraint on the cross-bridge cycling, it only follows that mutation or ablation of this protein has consequences for the contractility, the compliance and the relaxation of the myocardium. Accordingly, a significant increase has been observed in contractility and cross-bridge cycling rates in cMyBP-C -/- murine cardiomyocytes [8]. Paradoxically, at the whole-heart level contractile function is reduced in cMyBP-C -/- mice [7,8]. However, symptomatic HCM patients typically display a normal or elevated contractility except for those HCM patients who reached end-stage HCM, in which a decreased contractility and systolic dysfunction are characteristic [1]. A possible

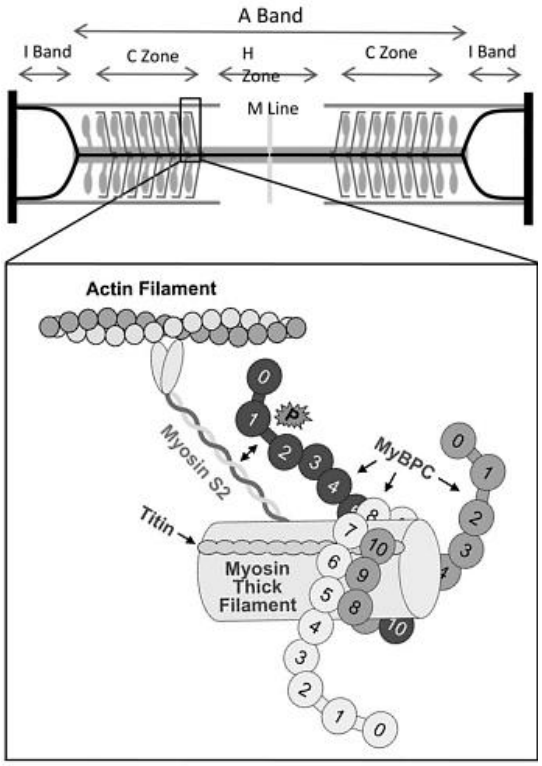


**FIGURE 1 Supposed arrangement of cMyBP-C in the cardiac sarcomere** The N-terminus ends supposedly interact with the myosin heads and actin [4] while the C-terminus ends are thought to either align parallel with the myosin thick filament or aggregate into a collar-like structure [5,8]. (Figure adapted and modified from Harris et al. 2011 [4] and Oakley et al. 2004 [37])

explanation for decreased whole-heart contractility, as opposed to increased cardiomyocyte contractility, is that according to the Frank-Starling law a reduced filling leads to a reduced power generation of the ventricle [8]. This would result in systolic dysfunction and hence reduced contractility.

Besides the mechanical function, it has been proposed that cMyBP-C has regulatory functions as well [3]. It is thought to play roles in PKA-mediated stretch activation and $Ca^{2+}$ sensitivity regulation [3]. Furthermore, the cMyBP-C phosphorylation sites are phosphorylated by PKA, PKC, PKD, CaMKII and ribosomal s6 kinase. Phosphorylation seems essential for the contractile function [3]. Moreover, it still remains unclear whether HCM hypertrophia is caused by haploinsufficiency or rather the formation of poison polypeptides. It has been shown that upon a myocardial infarct (MI) cMyBP-C undergoes a proteolytic cleavage, resulting in the presence of C0C1f fragments which would interfere with the proper function of wild-type cMyBP-C proteins [9]. A similar mechanism might also be responsible to some extent for the contractile dysfunction observed in HCM patients. It is also important to note that not all carriers of a cMyBP-C mutation necessarily present with HCM symptoms. This suggests that also other mechanisms must be involved in disease development.

## 1.2 Project design

### 1.2.1 Aims

The general aim of this research is to characterise the cMyBP-C-actin interactions *in vivo* as well as the way in which these interactions play a role in the onset and development of HCM. It is important to realise that there are unknown factors involved in HCM. The fact that not all MYBPC3 mutation carriers display HCM symptoms suggests that other yet to be identified mechanisms play a role. Hence, one should not only regard differences between HCM patients and healthy controls but also compare symptomatic and asymptomatic patients. In order to elucidate how cMyBP-C interacts with actin *in vivo*, an appropriate research model needed to be designed. Such a research model needs to both anticipate sufficient amounts of sample cells and minimise patient invasiveness and discomfort. Since *in vivo* derived cardiomyocytes would fulfill neither of these criteria, a model was needed in which cardiomyocytes are *in vitro* generated. Hence, an induced pluripotent stem (iPS) cell model was used to generate person-specific and genotype-specific cardiomyocytes that are representative for *in vivo* cardiomyocytes.

More specifically, this project aims at developing new tools that will enable a more detailed study of HCM as well as other cardiac diseases. Tools that are adressed in this project are the development of constructs for the use in Förster Resonance Energy Transfer (FRET) and the development of a functional reporter construct.

### 1.2.2 Hypotheses

In the future prospective of performing FRET experiments to determine and map the interactions between sarcomeric actin and cMyBP-C, fusion protein constructs were designed for both proteins. Importantly, at least one of the designed cMyBP-C constructs and a least one of the actin constructs should provide clearly detectable signals and should not interfere with actin-cMyBP-C interactions. This would allow the use of these constructs to compare wild-type iPS cell derived cardiomyocytes with iPS cell derived HCM cardiomyocytes. As a first step, we hypothesised that the designed constructs are correctly translated into functional fusion proteins. In order to test this hypothesis, 293T cells and HEK cells were transfected with the constructs, after which the fluorescence was imaged.

A second hypothesis was that CRISPR-Cas9 genome editing is an effective tool in the design of a reporter for cardiomyocytes. The primary idea is to design reporters for the cMyBP-C protein. However, as HCM patient iPS cell lines were not yet available, the functioning of the CRISPR-Cas9 tool was tested with the design a cardiomyocyte differentiation reporter construct. *Nkx2.5* is commonly used as a marker for cardiomyocyte differentiation, thus a *Nkx2.5*-RFP construct would provide an efficient imaging tool for cardiomyocyte differentiation. Using the CRISPR-Cas9 genome editing method, we integrated a RFP sequence in the genome of iPS cells right after the *Nkx2.5* gene but before its termination codon. This straightforward method allows to follow and to measure *Nkx2.5* expression by RFP imaging.

### 1.2.3 Objectives

In order to adress the first hypothesis, human fibroblasts needed to be reprogrammed into iPS cells. In the course of this project the iPS cell line SP11.1 was used as described and characterised by Sanchez-Danes et al. (2012) [10]. Afterwards, constructs were designed and

used for transfection in SP11.1 iPS cells. Fusion protein label constructs for *ACTC1*, which codes for actin, and *MYBPC3* were designed. In a final phase, these iPS cells needed to be differentiated into functional, beating and mature cardiomyocytes. Maturity is assessed by the presence of sarcomeres.

The first step in designing a CRISPR-Cas9 *Nkx2.5* reporter construct was to identify several candidate target sequences in the human genome. Thereafter, the cleaving efficiency of each sequence needed to be determined. Subsequently, iPS cells had to be transfected with Cas9, a donor RFP plasmid, and the appropriate gRNA. Finally, before differentiating into cardiomyocytes, the genomic integration of the plasmid needs to be verified.

### 1.2.4 Generation of iPS cell lines

In 2006, Takahashi and Yamanaka [11] identified four factors which are able to reprogram fibroblasts into so-called induced pluripotent stem cells (iPS). These four factors, more specifically *Oct3/4*, *Sox2*, *Klf4* and *c-Myc*, were retrovirally introduced in murine embryonic fibroblasts. Gene expression profiling of the derived iPS cells and embryonic stem (ES) cells revealed similarity between these cell types. Furthermore, teratoma formation and *in vitro* differentiation in the three germ layers indicated that the derived iPS cells were truly pluripotent and similar to ES cells [11]. In 2009, an alternative approach for iPS reprogramming was discovered [12]. Fibroblasts were transfected and reprogrammed with Sendai virus (SeV) vectors, each of which contained one of the four Yamanaka factors, i.e. *Oct3/4*, *Sox2*, *Klf4* and *c-Myc* **(Supplemental figure S5)**. This approach has several advantages [12,13]. Firstly, SeV vectors are not integrating into the genome and therefore are unlikely to induce genomic alterations. This reduces significantly the risk of tumourigenicity and genotoxicity. Also, Sendai virally iPS cell reprogramming requires a low multiplicity of infection (MOI). According to the Sendai reprogramming protocol set up by Invitrogen [14], each target cell is transfected averagely by three viron particles (MOI=3 CIU/cell)(Formula in *2.4 Sendai virus iPS cell reprogramming*). Another advantage is that these vectors and the exogenous transgenes can be removed from the target cells by single-colony subcloning until all colonies are negative for anti-SeV antibody staining [14]. Seven days after transduction, cells are seeded on top of irr-MEF or irr-HFF feeder cells [14]. Depending on the target cell type, iPS cell type colonies **(Figure 2)** should appear within four weeks after transduction. Typically, iPS cell colonies are characterised by compacted, elongated and triangular iPS cells. These cells are tightly aggregated in the colony. When the colony has grown bigger, the centre of the colony starts to give rise to differentiating cells due to cell-cell contacts. These centres are visible under the microscope as dense structures within the colony. When the colony has grown sufficiently to

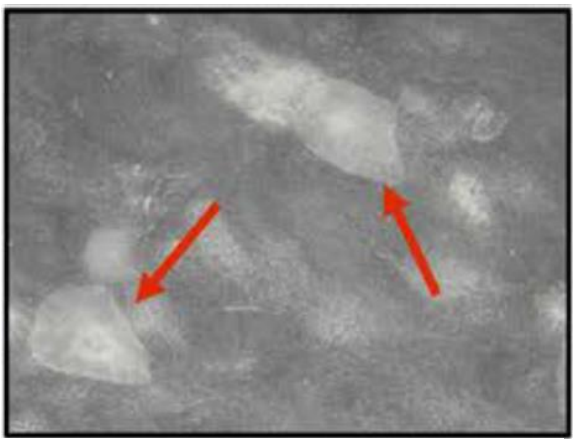

**FIGURE 2 iPS cell colonies** Within four weeks after transduction, colonies (arrows) should start appearing. Note the denser centre of differentiating cells.

.

perform a split, one should avoid using these colony centres for the split. In order to maintain and keep the quality of the cell line, one should keep splitting these iPS cell colonies on top of feeder cells. However, when planning to use the iPS cells for an experiment, it is more convenient to passage the iPS cells feeder-free. iPS cells are then passaged on Matrigel-coated (Matrigel from Corning, Cat. 354234) plates and fed with conditioned HES medium. In order to condition hES medium, one adds this medium to MEF feeder cells for at least 24 hours. During this period the MEFs supplement the medium with LIF and essential both known and unknown cytokines [15,16]. iPS cells need these factors as well as a suitable substrate in order to survive and grow. Fibroblasts can be a good substrate for iPS cells. In absence of these fibroblasts, the Matrigel is needed to provide a substrate.

Once the iPS cells of this project were in a feeder-free culture, they were transfected with vectors containing the fusion genes. In a parallel experiment iPS cells were transfected with the *Nkx2.5*-RFP construct. Since the C-terminal and N-terminal ends of a protein are usually situated on the exterior, these are the first options to be considered for the placement of a fusion protein label. Hence, an *MYBPC3*-GFP construct, a GFP-*MYBPC3* construct, an *ACTC1*-RFP construct and a RFP-*ACTC1* construct were designed. The iPS cells were selected for presence both an MYBPC3 construct and an actin construct.

### 1.2.5 Differentiation into cardiomyocytes

After selection of the iPS cells for presence of both a cMyBP-C construct and an actin construct, the iPS cells were differentiated into cardiomyocytes. There are several ways to obtain cardiomyocyte differentiation. A first method is to grow embryoid bodies (EB). EBs are *in vitro* aggregates of either ES cells or iPS cells. When these EBs are formed from true pluripotent stem cells, they subsequently differentiate into cell types of all three germ layers, including cardiomyocytes. However, only a minimal cardiomyocyte differentiation of 1% has been observed in EBs [17]. Another method includes the use of Activin and BMP4 to enhance cardiomyocyte differentiation in both EBs [18] and ES cell monolayers [19]. The method with the largest differentiation efficiency follows a small molecule-based approach [17]. It has been shown that the Wnt/ß-catenin pathway **(Supplemental figure S6)** induces cardiogenesis and haematopoiesis in a biphasic and opposite manner **(Supplemental figure S7)**[17,20,21]. Early Wnt/ß-catenin pathway activation and late Wnt/ß-catenin pathway inhibition has proven to maximise cardiomyocyte differentiation [17]. In the so-called GiWi protocol which was used for this project, pluripotent stem cells are first exposed to CHIR99021 (Selleckchem, Cat. CT99021) which is a Gsk3 inhibitor and hence a Wnt/ß-catenin pathway activator. In a later stage of differentiation the intermediate cells are exposed to IWP-4 (Stemgent, Cat. 24804-0036) which inhibits Wnt production and thus autocrine and paracrine activation of the Wnt/ß-catenin pathway.

### 1.2.6 CRISPR-Cas9 genome editing

As mentioned above, an *Nkx2.5*-RFP construct was designed and integrated into the genome of the iPS cells by means of CRISPR-Cas9 genome editing. This technique is based on an acquired bacterial defence mechanism against viral DNA. Clustered regularly interspaced short palindromic repeats or CRISPRs are present in about 40% of bacterial genomes [22] and are often preceded by CRISPR-associated (Cas) genes. Cas genes are involved in the recognition of invading foreign DNA and producing a novel palindromic repeat sequence in the CRISPR region. Upon a second infection with the same DNA sequence, the bacterial defence response includes the transcription of the CRISPR sequence, which is subsequently cleaved and

processed into mature crRNAs. Cas genes form complexes with the mature crRNAs which then serve as a recognition template for the invading foreign DNA. Subsequently the associated Cas protein cleaves the invading DNA and hence prevents viruses from replicating inside the bacteria, altering genomic DNA or exerting toxicity **(Supplemental figure S9)** [22].

In order to insert a sequence one needs to create a double-strand break (DSB) at the desired location in the genome of the target cells. A cell's response to a double-strand break is either to repair this break by non-homologous end-joining (NHEJ) or homology-directed recombination (HDR). NHEJ occurs most frequently and generates indel mutations at the site of the DSB [23,24]. However, HDR occurs to some extent whenever a repair template sequence containing homology arms is present. The CRISPR-Cas9 system II can be used to introduce a DSB at the desired location in the genome. Subsequently, the target cell recombines the homology arms of the repair sequence with the DSB upstream and downstream genome sequences. In order to select and create a DSB with the Cas9 endonuclease, one first needs to design an oligonucleotide sequence complementary to a target sequence in the genome which is followed by a protospacer-adjacent motif (PAM) sequence. For instance, in this project Cas9 originates from *Streptococcus pyogenes* and recognises sequences with a G-19-NGG pattern. In this pattern a guanine and its 19 following nucleotides compose the target sequence for which a complementary sequence needs to be designed. This complementary sequence is called the crRNA sequence. The tracrRNA sequence is a hairpin RNA sequence that connects the crRNA with the Cas9 endonuclease. The guide RNA or gRNA is the collective name for the crRNA and the tracrRNA. In the newer CRISPR-Cas9 systems, the tracrRNA is already included in the gRNA vector and the gRNA is expressed as one sequence. Cas9 and its associated gRNA need a PAM sequence in order to recognise the cutting sites. For *streptococcus pyogenes* originated Cas9 this PAM sequence is NGG. Upon creating the desired DSB, HDR will cause integration of any repair sequence that contains homology arms [23,24]. In this project the CRISPR-Cas9 system II was used to integrate an RFP sequence right before the termination codon of *NKX2.5*, such that expression of RFP coincides with *NKX2.5* expression. Since NKX2.5 is a marker for cardiomyocyte differentiation, one can visualise cardiomyocyte differentiation by means of RFP imaging.

### 1.2.7 Planned future experiments

Once iPS-derived cardiomyocytes are obtained, several techniques can be considered in order to investigate the interactions between actin and cMyBP-C. At least two of these techniques, Förster Resonance Energy Transfer (FRET) and dynamic cell traction force microscopy, are planned in the context of this research but are beyond the scope of this specific project.
FRET is a technique that is based on the non-radiative energy transfer between two fluorescent labels. In order to use this technique, actin was labelled with RFP and cMyBP-C was labelled with GFP. When a GFP molecule is excited and is sufficiently close to a RFP molecule, part of the energy absorbed by the GFP molecule transfers to the RFP molecule. The RFP molecule absorbs this latter energy, resulting in the excitation of an outer electron. After relaxation of this electron, the RFP molecule emits a photon. The intensity of the RFP emission can be used to calculate the distance between the GFP molecule and the RFP molecule. This calculated distance will aid in understanding how cMyBP-C and sarcomeric actin interact.
A second technique which will be used is dynamic cell traction force microscopy. This is a rather robust technique, which will allow measuring the forces developed by cardiomyocytes. Ideally there will be no significant difference between cardiomyocytes that are not transfected with the constructs and those that are. In a later phase, this technique will also be used to compare forces produced by human HCM iPS-derived cardiomyocytes and wild-type healthy controls.

# 2. Materials and methods

## 2.1 Reagents

| | |
|---|---|
| HDF medium | DMEM (without glutamin)(Gibco, Cat. 41966052), 10% FBS (Hyclone, Cat. 16V30160-03), 2mM UltraGlutamine 1x (Lonza, Cat. BE17-605E/U1), 50U/ml penicillin/streptomycin 100x (Lonza, Cat. DE17-620EI) |
| hES medium | KO-DMEM (Gibco, Cat. 10829018), 20% KOSR (Gibco, Cat. 10828-028), 2mM UltraGlutamine, 50U/ml penicillin/streptomycin, 1% NEAA 100x (Lonza, BE13-114E), 0.1% ß-mercaptoethanol (50nM, Gibco, Cat. 31350-010), 0.01% bFGF (100µg/ml stock, Peprotech) (hES medium becomes conditioned when it is added to MEFs for at least 24 hours, during which it is supplemented with essential cytokines and LIF.) |
| HFF medium | IMDM (Gibco, Cat. 21980-032), 10% FBS, 2mM UltraGlutamine 100x, 50U/ml penicillin/streptomycin |
| Keratinocyte medium | DMEM, DMEM/F12, FBS, RM+ 100x, 2mM UltraGlutamine 100x, 50U/ml penicillin/streptomycin |
| RM+ 100x | 500µg/ml transferrin, 40µg/ml hydrocortisone, $10^{-8}$M cholera toxin, 1µg/ml EGF, 500µg/ml insulin, $1.77x10^{-9}$M liothyronine |
| Differentiation medium | KO-DMEM, 20% FBS, 2mM glutamine, 0.1 mM ß -mercaptoethanol, 1% NEAA 100x, 50U/ml penicillin/streptomycin |

## 2.2 Derivation of primary cell cultures

Dermal punch biopts were obtained from healthy volunteering control subjects as well as from two HCM patients, who all signed a written informed consent. Dermal layers were separated from the adipose tissue and cut into smaller pieces with about a millimetre diameter. Explants were set up for both keratinocytes and dermal fibroblasts. For explanting keratinocytes, skin pieces were cultured in a specific keratinocyte medium. For explanting dermal fibroblasts, skin pieces were cultured in HFF medium. Explants were cultured until the evading fibroblasts and keratinocytes obtained a confluency of 80-90%, which is the time point at which the cells should either be passaged or subjected to iPS cell reprogramming. Keratinocytes were subsequently frozen for later usage.

## 2.3 Retroviral reprogramming

A control iPS cell line was established and named SP11.1. Phoenix-Ampho (ϕNX-A) cells (ATCC, Cat. CRL-3213) were transfected with retroviral plasmids containing three of the four Yamanaka factors, i.e. pMSCV-hOCT4 (Addgene, 20072), pMSCV-hSOX2 (Addgene, 20073) and pMSCV-hKLF-4 (Addgene, 20074). Transfection was carried out with X-tremegene 9 DNA

Transfection reagent (Roche, Cat. 06365779001). After 24 hours media were changed to HDF medium solely. After another 24 hours these media were supplemented with the vectors produced by the ϕNX-A cells. These vector-supplemented media were harvested and added to the biopt-derived dermal fibroblasts (3 x 1ml of media, each containing one of the three Yamanaka factors). After 2-3 days, target cells were seeded on top of irradiated neonatal human foreskin fibroblasts (HFF) (ATCC, Cat. CRL-2429).

## 2.4 Sendai virus iPS cell reprogramming

Dermal fibroblasts of the HCM patients were cultured in a 6-well plate to a confluency of 80-90%. In this stage, the fibroblasts are ready for transduction. Sendai viral vectors, each of which containing one of the four Yamanaka factors (CytoTune Sendai hOct3/4, CytoTune Sendai hSox2, CytoTune Sendai hKlf4 and CytoTune hc-Myc), were purchased from LifeTechnologies™. HFF medium was enriched for 24 hours with $3.10^6$ CIU of each SeV vector. Eight days after transduction, transduced cells were removed by 0.05% Trypsin/EDTA and seeded on top of irradiated human foreskin fibroblasts (HFF). Important for the reprogramming is the application of a sufficient amount of viral vectors such that MOI = 3 CIU/cell. The MOI is calculated with formula 1.

$$MOI = \frac{Ccp \times Vcp \times Vw}{Vd \times Nw} \qquad (1)$$

*Ccp is the viral vector concentration in the commercial package (CIU/ml), Vcp is the volume taken out of this commercial package (ml), Vw is that part of the dilution volume that is added per well (ml), Vd is the dilution volume (ml), i.e. the volume of fibroblast medium in which the viral vectors are diluted and Nw is the number of cells per well (cells).*

## 2.5 iPS cell culturing on top of feeder fibroblasts

Retrovirally or Sendai-virally derived iPS cells were cultured on top of HFF feeder layers for 7 days until the cells are ready to be split. Two days before the cells were split, a Matrigel-coated plate had been seeded with irr-HFFs in HFF medium at a density of $4.10^6$ cells per 100mm dish. Two hours before splitting, this medium was removed and the plate was washed and then refilled with hES medium. The iPS cell colonies were picked with a Stripper micropipette and seeded on top of the irr-HFFs in the new plate. iPS cells were cultured and passaged on feeder cells several times before they were passaged in a feeder free culture.

## 2.6 Feeder-free iPS cell culturing

In order to provide the iPS cells with a substrate that mimicks the *in vivo* extracellular matrix, plates were coated with Matrigel. iPS cells were picked from their colonies on the HFF layer and seeded in these Matrigel-coated plates with conditioned human embryonic stem cell medium (hES-CM). hES-CM was produced by irradiated mouse embryonic fibroblasts (irr-MEF) which were seeded in gelatin-coated (0.1% Ultrapure water with gelatin, Millipore, Cat. E5-006-B) plates and cultured with hES-medium. MEFs originated from CD1 mice. The conditioned medium was collected each 24 hours and replaced with new hES-medium.

iPS cells were grown until the colonies reached an 80-90% confluency, after which they were detached and disaggregated by means of accutase (eBioScience, Cat. 00-4555-56). iPS cells were 10 times diluted, reseeded in a Matrigel-coated plate and fed with hES-CM.

## 2.7 SP11.1 iPS cell line characterisation

### 2.7.1 Alkaline phosphatase staining

Alkaline phosphatase stainings were performed in order to mark undifferentiated cells. IPS cell culture plates were washed twice with PBS 1x and incubated for 2-3 minutes at room temperature with a fixing solution (3.7% paraformaldehyde in PBS 1x). Subsequently, the culture plates were washed with a membrane substrate solution (50% Solution A and 50% Solution B from Sigma Blue AB0300-1KT). Then the plates incubated for 20 minutes at room temperature in the dark with the substrate solution. The substrate solute solution was removed and PBS 1x was added.

### 2.7.2 Transgene silencing

The expression of transgene retroviral Yamanaka factors in the SP11.1 iPS cell line needs to be silenced in order to establish a well-reprogrammed iPS cell line [25]. In order to establish a silenced expression for the transgenes and an increased expression of the endogenous pluripotency genes, an RT-PCR was performed. Obtained expression values were normalised to the GAPDH expression.

### 2.7.3 Karyotype

Firstly, a plate of SP11.1 iPS cells was prepared for karyotyping by adding Colcemid. Colcemid inhibits the mitotic cycle at the metaphase stadium. Then, a hypotonic solution was added to increase cellular volume and to facilitate unfolding of the chromosomes. Subsequently, the cells were fixed with a mixture of methanol and acetic acid (3:1). The karyotype of the SP11.1 cell line was then performed by an external laboratory.

### 2.7.4 Pluripotency markers

Pluripotency of the derived iPS cells was validated by staining three nuclear and three surface markers for pluripotency. Nuclear markers for pluripotency in iPS cells are *Nanog*, *Oct4* and *Sox2*. Surface markers for pluripotency in human iPS cells are *Tra-1-81*, *SSEA-3* and *SSEA-4*. Additionally, all nuclei were stained by DAPI. Staining was performed on iPS cells on top of feeder fibroblasts.

### 2.7.5 *In vitro* differentiation

Embryoid bodies (EBs) were derived from the SP11.1 cells by putting them in a 96-well plate with 20,000 to 30,000 cells per well and centrifuging this plate in order to aggregate the cells. Afterwards, the resulting embryoid bodies were differentiated into cells of the three germ layers. Endodermal differentiation was achieved by adding differentiation medium. Mesodermal differentiation was induced by providing the cells with differentiation medium and ascorbic acid. Ectodermal differentiation was induced by coculturing the SP11.1 iPS cells with stromal cells. Subsequently, endodermal cells were stained for α-fetoprotein and FOXA2. Mesodermal cells were stained for smooth muscle actin (SMA) and ectodermal cells were

stained for Tuj1. Additionally, the nuclei of differentiated cells from all germ layers were stained with DAPI.

### 2.7.6 DNA methylation

DNA methylation of five CpG islands in the promotor sequences of *Nanog* and *Oct3/4* was measured by means of bisulphite sequencing. *Nanog* and *Oct3/4* promotor demethylation are frequently regarded as characteristic hallmarks for induced pluripotent stem cells [26].

### 2.7.7 Teratoma formation

In order to verify *in vivo* whether the obtained iPS cells are able to differentiate into cells of all three germ layers, iPS cells were injected into the testes of severe combined immunodeficiency (SCID) mice. After 6-8 weeks, the mice were sacrificed. Tumour tissue was resected and stained for two markers of each germ layer. Endodermal cells were stained with α-fetoprotein and *FOXA2*. Mesodermal cells were stained for chondroitin sulphate and *Sox9* and ectodermal cells were stained for *Tuj1* and *GFAP*. Additionally, all cells were stained with DAPI.

## 2.8 Construct design

Four fusion gene constructs in a pcDNA3 vector were designed for the FRET analysis, i.e. *ACTC1*-RFP fusion gene, RFP-*ACTC1* fusion gene, *MYBPC3*-GFP fusion gene and GFP-*MYBPC3* fusion gene. cDNA sequences of sarcomeric actin and cMyBP-C were derived from human vesicular mRNA in a previous research project. The goal is to transfect iPS cells with combinations of these constructs in such a way that all transfected iPS cells contain both a vector with sarcomeric actin and a vector with *MYBPC3*. Since the RFP and GFP labels are either C-terminally or N-terminally fused, four possible combinations can be made. In order to select for iPS cells that contain two vectors, i.e. one with an actin fusion gene and one with a *MYBPC3* fusion gene, two different selection cassettes are required. The original neomycin resistance cassette of the pcDNA3 vector (**Supplemental figure S10**) was kept for the *MYBPC3* fusion gene constructs. In the actin fusion gene constructs, this neomycin resistance cassette was replaced with a puromycin resistance cassette. In order to do so, the neomycin resistance cassette was removed by cleaving and subsequent blunting of the Sma1 and Bsm1 restriction sites. Next, the puromycin resistance cassette was removed from the pPuro commercial vector (**Supplemental figure S11**) by cleaving and subsequent blunting of the HindIII and BamHI restriction sites. The puromycin resistance cassette was then ligated into the pcDNA3 vector (**Supplemental figure S12**). Since blunt-ended fragments can insert in two directions, a PCR was performed to select the vectors with the correct insertion. The fused genes in these four constructs were connected with a linker sequence, allowing for the fusion proteins' components to remain fused after translation. The MYBPC3 fusion gene constructs were already synthesised before the start of this project.
In contrast, a *NKX2.5*-RFP construct was designed without a joining linker sequence, but with a 2A sequence as described by Ryan et al. 1991 [27] and Kim et al. 2011 [28]. This 2A sequence encodes a self-cleaving protein which causes the NKX2.5 and RFP proteins to separate.

### 2.8.1 Polymerase chain reaction

Nucleotide sequences of RFP and actin were amplified by a polymerase chain reaction (PCR) with Phusion DNA Polymerase (Thermo Scientific) and Phusion HF buffer (Thermo Scientific). In order for the PCR fragments to contain unique restriction sites at their distal ends, restriction enzymes were determined that do not cleave within the nucleotide sequence. Then, PCR primers were designed in a way that the first two primer nucleotides are adenosines, the purpose of which is to buffer eventual primer degradation. These adenosines are followed by the target sequence of the restriction enzyme that does not cut in the gene sequence. This target sequence is in turn followed by the first twenty-some nucleotides of the coding exon sequence of one of the four proteins. However the number of the latter nucleotides may vary since they ideally should have a 50% GC-content and an annealing temperature of around 60°C. The gene being fused at the C-terminal end additionally contains a linker sequence ACTAGTGGC. This linker sequence will allow for both proteins to be expressed while remaining attached to each other. All sequences were amplified by PCR.

### 2.8.2 Gel electrophoresis

After PCR amplification of the sequences, a gel electrophoresis was performed in order to visualise and purify the PCR fragments and the selection cassettes used. Cells were selected for the presence of two different vectors, of which one contains *MYBPC3* and GFP and the other sarcomeric actin and RFP. Hence, it is necessary to use two different selection cassettes. The vectors with *MYBPC3* and GFP have a selection cassette that induces neomycin and geneticin resistance. The vectors with sarcomeric actin and RFP have a selection cassette that induces puromycin resistance. The fragments were visualised by ethidium bromide.

### 2.8.3 Gel extraction of the actin, cMyBP-C, GFP and RFP constructs

The bands of the four sequences were cut out of the electrophoresis gel and the DNA polymers were extracted by means of the GeneJET Gel Extraction Kit (ThermoScientific, LOT. 00208492). The gel pieces were incubated for 10 minutes at 50°C with the Binding Buffer (1µl per mg of gel) of this kit. The resulting solutions were then purified by centrifugation through GeneJET purification columns. Afterwards, the GeneJET purification columns were washed with the Wash Buffer of this kit. The Elution Buffer was used to catch the DNA sequences from the filter in the purification columns.

### 2.8.4 Ligation into the pcDNA3 vector

The pcDNA3 vectors and the PCR fragments were digested with the selected restriction enzymes. For the MYBPC3-GFP construct, MYBPC3 was digested with *KpnI* and *BamHI* and GFP was digested with *BamHI* and *EcoRI*. Conversely for the GFP-MYBPC3, GFP was digested with *KpnI* and *BamHI* and MYBPC3 was digested with *BamHI* and *EcoRI*. The pcDNA3 vectors for the MYBPC3 constructs were digested with *KpnI* and *EcoRI*.
Analogously for the ACTC1-RFP construct, ACTC1 was digested with *HindIII* and *BamHI* and RFP was cleaved by *BamHI* and *EcoRI*. For the RFP-ACTC1 construct, RFP was digested with *HindIII* and *BamHI* and ACTC1 was digested with *BamHI* and *EcoRI*. The pcDNA3 vectors intended for the ACTC1 constructs were digested with *HindIII* and *EcoRI*. After the digestions, the PCR fragments were ligated into the respective vectors by means of T4 ligase.

### 2.8.5 Amplification by transforming Escherichia Coli DH5

Vectors were thawed at room temperature and subsequently added to *Escherichia Coli DH5* bacteria. Bacteria were kept on ice for 30 minutes, after which a thermic shock was applied. Afterwards, bacteria were put shortly on ice and then incubated on a Thermomixer for one hour at 37°C. Lastly, bacteria were plated on an agar plate and incubated overnight. The day after a single, clearly defined colony was picked from the agar plate and cultured and amplified in a bacterial culture tube.
Bacteria were lysed and plasmids were subsequently extracted by means of the NucleoSpin® Plasmid EasyPure kit from Macherey-Nagel (Ref. 740727.250). Vectors were diluted to 1µg/µl.

### 2.8.6 Testing of vector transfection efficiency

Efficiency of the designed ACTC1 vectors was tested in 293T cells in a 24-well plate. The MYBPC3 vectors were previously tested in HEK293 cells, since 293T cells already contain a neomycin resistance cassette acquired by the transformation of this cell line. Cells were detached with Trypsin/EDTA 0.05% (Gibco, Cat. 25300-054), pipetted to disaggregate all clumps and subsequently diluted in HFF medium. Each well was seeded with 80,000 cells of this single-cell suspension. After 24 hours cells were transfected with 1.25µg/ml, 2.50µg/ml, and 3.75µg/ml of the vector tested. A double transfection control was included, in which cells were transfected with both 1.25µg/ml of the respective construct and 1.25µg/ml of a control vector. The control vector for the actin constructs was GFP and the control vector for the cMyBP-C constructs was mCherry. Vectors were resolved in 150 mM NaCl (pH5.5) and 5% polyethylenimine (PEI) (Polysciences Inc., Cat. 24756-2) in a total volume of 50µl. This solution was incubated for 10 minutes at room temperature and subsequently added dropwise to the cells. After 24 hours, cells were selected for the presence of a construct, i.e. HEK293 cells transfected with one of the vectors containing MYBPC3 and a neomycin resistance cassette were selected with 800µg/ml geneticin, which is a neomycin sulphate analog. Analogously, 293T cells that were transfected with one of the vectors containing ACTC1 and a puromycin resistance cassette were selected with 2.5µg/ml puromycin.
For all cell groups, the medium was replaced daily and every other day the medium was enriched with the respective antibiotic. As soon as cell death was observed, fluorescence pictures were taken with an inverted microscope.

## 2.9 Vector transfection and selection

Four groups of iPS cells were assigned and grown on Matrigel and fed with conditioned hES medium. Subsequently, each group was transfected with one of the four fusion gene constructs by means of the Xtremegene-9 transfection reagent. Cells were transfected by adding a mixture of 900µl Optimem, 27µl Xtremegene-9 and 9µg of the respective vector. CMyBP-C-encoding vectors contained a neomycin resistance cassette. Hence, cells transfected by one of these vectors were selected by supplementing their conditioned hES medium daily with 50µg/ml geneticin (Sigma, Cat. G-418), starting 48 hours post-transfection. Conversely, actin-encoding vectors contained a puromycin resistance cassette. Cells transfected with one of the actin-encoding vectors were selected by supplementing the hES-CM with 2µg/ml puromycin. Once apoptosis was no longer observed, iPS cells of each MYBPC3 group were selected, reseeded and expanded in two new Matrigel-coated 100mm dishes per MYBPC3 group. One dish will later be transfected with the *ACTC1*-RFP construct while the other dish will be transfected with the RFP-*ACTC1* construct. The resulting four groups of transfected iPS cells will also be selected as of 48 hours post-transfection with both geneticin and puromycin

(Sigma, Cat. P8833-10MG) for a duration of another two weeks. Geneticin concentration in the medium will as well be 50µg/ml and puromycin concentration was 2µg/ml. Subsequently, iPS cells will be expanded and differentiated into cardiomyocytes. The antibiotic selection was applied daily to the iPS cells. The initial two ACTC1 groups will be stored and kept for later validation of the construct.
In parallel, four other groups other groups of iPS cell transfections were made. Each of these groups was transfected with a combination of an MYBPC3 and an ACTC1 construct. These groups were transfected with a mixture of 900µl Optimem, 27µl Xtremegene-9 and 4.5µg of the respective MYBPC3 and ACTC1 construct. These four groups were daily selected with 50µg/ml geneticin and 2µg/ml puromycin.

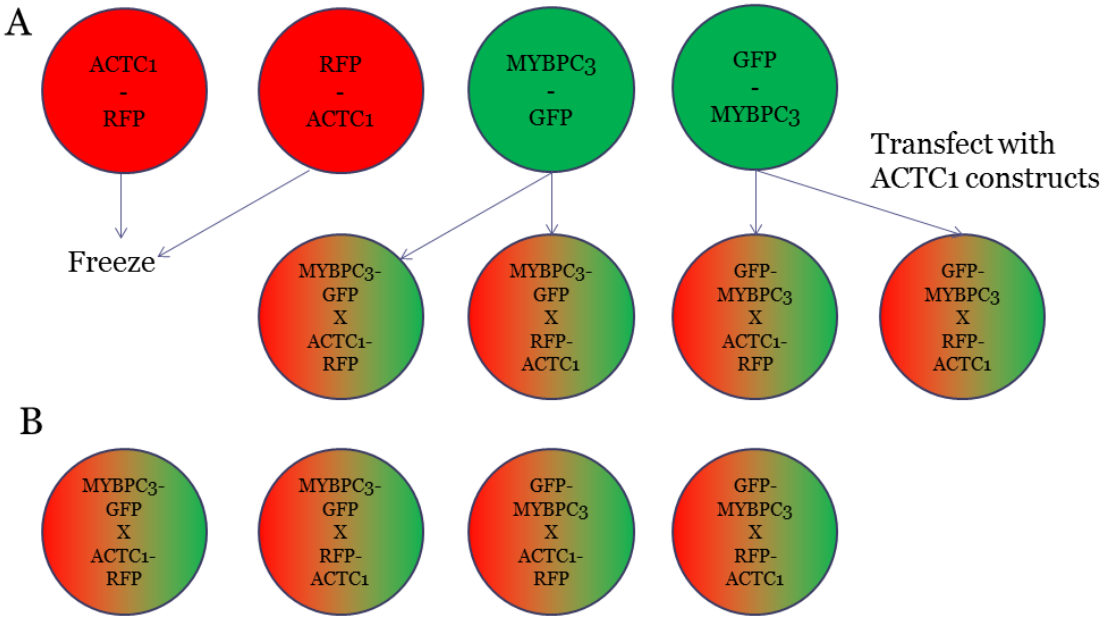


**FIGURE 3 Scheme of all transfection groups. A.** Four groups were assigned in which iPS cells were only selected with one of the four constructs. The MYBPC3 construct groups will after selection be transfected with each of the ACTC1 constructs as well. The ACTC1 construct groups will be frozen after selection. **B.** Four other groups were assigned in which each group was transfected with one of the MYBPC3 constructs and one of the ACTC1 constructs.

A control iPS cell line (kiPS3F7) was differentiated into cardiomyocytes using the GiWi protocol as described by Lian et al. 2013 [17]. On day -3 of this protocol iPS cells were seeded at a density 150,000 cells per well in a 12-well plate coated with Matrigel. Culture medium consisted of mTeSR (Stemcell Technologies, Cat. 05850) with 0.1% ROCK inhibitor (10mM, Miltenyi Biotech). The next two days the medium consisted only of mTeSR. On day 0 cells were cultured with RPMI (Lonza, Cat. L0501-500)/B27 without insulin (Gibco, Cat. A18956-01) and a GSK3 inhibitor (CHIR99021, Selleckchem, cat. S1263-25mg) at a concentration of 1.2µl/ml. For the next two days, cells were cultured in the same medium without the GSK3 inhibitor. On day 3 a Wnt-inhibitor was added to the same medium (1µl/ml) and cells were incubated with this inhibitor for 48 hours. At day 5 medium was replaced by solely RPMI/B27 without insulin. On day 7 and on every 2-3 following days, medium was replaced with RPMI/B27 with insulin (Gibco, Cat. 17504-044). Beating cells should appear between day 8 and 12.

## 2.11 IPS cell-derived cardiomyocyte immunostaining

In order to test the newly purchased antibody for cMyBP-C (Santa Cruz Biotech), iPS cell-derived cardiomyocytes were stained. The cardiomyocytes were fixed with 4% paraformaldehyde (PFA) and washed with Tris-buffered saline (TBS). Subsequently, they were incubated for 72 hours at 4°C with a mouse primary antibody for cMyBP-C, namely MYBPC3 (G-1) (1:50, Santa Cruz Biotechnology, Inc., sc-137182), and rabbit Troponin I Antibody (H-170) (Santa Cruz Biotechnology, Inc., sc-15368). Primary antibodies were diluted 1:50 in TBS + 0.1% Triton-X + 6% donkey serum. After washing with TBS+0.1% Triton X-100 and blocking with TBS+0.1% Triton X-100+6% donkey serum, the cardiomyocytes were incubated for 2 hours at room temperature with secondary antibodies. The secondary antibodies were Cy™2 AffiniPure Goat Anti-Mouse IgG (1:500, Jackson ImmunoResearch Laboratories, Inc.) for cMyBP-C and Cy™3 AffiniPure Donkey Anti-Rabbit IgG (1:500, Jackson ImmunoResearch Laboratories, Inc.). After washing with TBS+0.1 Triton X-100 and TBS, the cardiomyocytes were stained with DAPI (1:5000 in TBS+0.3% Triton X-100 + 6% donkey serum). Cardiomyocytes were mounted in a solution of polyvinyl alcohol (PVA) and DABCO.

## 2.12 CRISPR-Cas9 genome editing

In parallel, a CRISPR-Cas9 experiment was conducted in order to generate cardiomyocytes with an RFP expression coupled to *Nkx2.5* expression. In order to use the Cas9 enzyme, a suitable gRNA needed to be identified. The *Nkx2.5* locus was examined and the three gRNA candidates closest to the stop codon were selected and PCR primers were ordered to amplify these candidate sequences. PCR primers were designed in such a way that a BsmBI restriction site was included in the sequences, in order to ligate the candidate gRNAs into vectors.
Then, the most efficient gRNA of these candidates was selected by means of a T7E1 assay. Each of the three gRNAs was transfected into 293T cells using PEI as a transfection reagent, analogous to the PEI transfection described in *2.9 Vector transfection and selection*. At this point the Cas9 enzyme had introduced a DSB in a subset of each sample, leading to indel formation (**Figure 4A**). Afterwards, 293T cells of each condition were centrifugated and the genomic DNA was extracted. PCR primers were designed in such a way that the PCR product was approximately 600bp long with the Cas9 cleavage site in the middle. The PCR was performed and afterwards the T7E1 enzyme and New England Biolabs buffer (NEB buffer) were added. After the PCR reaction all strands are amplified and rehybridised (**Figure 4B**). Subsequently, the cleavage reaction was carried out in a PCR machine during 15 minutes at 37°C. The T7E1 enzyme recognises mismatched sequences. Hence, all heteroduplex dsDNA strands were cut by T7E1 (**Figure 4C**). Afterwards, loading dye was added to each sample and gel electrophoresis (2% agarose) was carried out. Bands were visualised and band intensities were measured. Intensities correlate directly with the amount of DNA present in the respective bands. In order to calculate efficiencies of the cleavage reactions for each of the gRNAs, we derived the x-axis intercepts of equation 2. More conventionally, cleavage efficiencies are approximated with formula 3.

$$E^2 - E + \frac{a}{2} = 0 \qquad (2)$$

*with $E$ the cleavage efficiency and $a$ the band intensity of the cleaved DNA*

$$E = 1 - \sqrt{1 - a} \qquad (3)$$

with $E$ the cleavage efficiency and $a$ the band intensity of the cleaved DNA

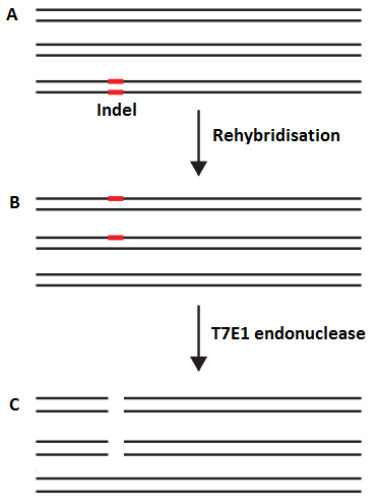


**FIGURE 4 General scheme of the T7E1 assay. A**. The Cas9 enzyme cleaved a fraction of the target sequences of all 293T cells in the sample. **B.** DNA was amplified and strands reannealed randomly. **C.** The T7E1 endonuclease cleaved the resulting mismatch heteroduplexes. Subsequently, the DNA fragments were separated by gel electrophoresis. (Figure adapted and modified from [38])

After the T7E1 assay and selecting the most efficient gRNA, iPS cells were expanded in a 150mm plate till a state of approximately 80% confluency was reached. Four hours before transfection, the medium was supplemented with ROCK inhibitor (1:1000). Two transfection methods were tried.

A first transfection was carried out by electroporation. For this electroporation, the medium from the plate with iPS cells was removed and the plate was washed with PBS. Subsequently, accutase was added to detach the iPS cells. Cells were washed with hES medium to inactivate the accutase, after which the pellet was resuspended in a small volume of medium (100-200µl). Cells were counted and $10^6$ cells were put in an electroporation cuvette (4mm cross-section) together with a transfection mixture. The transfection mixture for the electroporation method consisted of 700µl PBS, 21µg Cas9 plasmid (**Supplemental figure S13**), 7µg of gRNA plasmid (**Supplemental figure S14**), 35µg of the designed *Nkx2.5*-RFP construct and 0.8µl of ROCK inhibitor. The cuvette was placed into an electroporation machine and electroporation was performed. Afterwards, the transfected iPS cells were reseeded in a Matrigel-coated 150mm plate.

The second transfection was mediated by the FugeneHD transfection reagent. The transfection mixture for this transfection consisted of 800µl of KO-DMEM, 6µg of the *Nkx2.5*-RFP construct, 3.75µg of of the Cas9 plasmid, 1.25µg of gRNA3, and 1.50µg of pRFP, which is a control vector. This mixture was then supplemented with 37.5µl Fugene®HD (Promega, Ref. E2311). After 15

minutes of incubation at room temperature, this mixture was added dropwise to a 100mm plate of control iPS cells.
After 48 hours and every following day, the media of all transfected iPS cells were changed to new cHES medium supplemented with geneticin (1:1,000) and ganciclovir (2µM) in order to select for transfected cells.

# 3. Results

## 3.1 Derivation of primary cell cultures

In order to establish patient-specific iPS cell lines, primary cell cultures were derived from two HCM patients, one of which is symptomatic for HCM. As we expected, the explants that were cultured in keratinocyte medium showed an outgrowth of primarily keratinocytes (**Figure 5A-C**). We obtained typical keratinocytes with a small, hexagonal morphology as depicted in **Figure 5A-C**. Accordingly, explants cultured in fibroblast medium displayed an outgrowth of fibroblasts (**Figure 5D-F**). The obtained fibroblasts all showed typical elongated cell morphology.

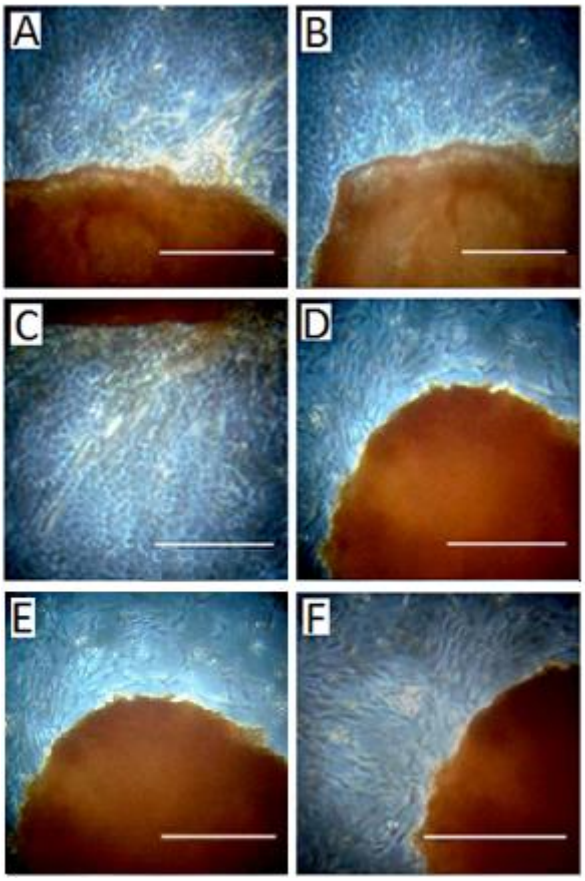


**FIGURE 5 Explants (Scale bars = 500µm)** Both explants in keratinocyte medium (A-C) and HFF medium (D-F) were set up. Keratinocytes are characterised by small hexagonal cells. In these explants also fibroblasts were cultured (not visible). In the explants for fibroblasts elongated spindle-shaped cells were observed.

## 3.2 Sendai iPS reprogramming of HCM patient-derived fibroblasts

The fibroblasts derived from two HCM patients were seeded into non-coated 100mm plates. After the Sendai-viral reprogramming, apoptosis was observed (**Figure 6**). This apoptosis is normal after any iPS reprogramming event and can be used as an indication for the transduction effectiveness. Cells acquired a more rounded shape, instead of the typical

elongated fibroblast shape. They also seemed less compacted. Reprogrammed fibroblasts were cultured in the same plates during eight days, at the end of which they grew to a state of near-confluency. Then, all cells were reseeded on top of HFF feeder fibroblasts.
One week after reseeding, colony-like structures of small cells were observed (**Figure 7**). These are not iPS cell colonies, but these structures consist mainly of partially reprogrammed and partially dedifferentiated cells. Only after two to four weeks, the actual iPS cell colonies start to appear. Since the patient-derived iPS cells were not ready yet, we show an image from another cell line (**Figure 8**).

## 3.3 iPS cell cultures

After colonies appeared on top of the feeders, iPS cells were passaged several more times on new feeders. Thereafter, the iPS cells were cultured in a Matrigel-coated plate and fed with hES-CM. The first day after seeding the iPS cells in Matrigel-coated plates, small cell clusters were observed. This observation was similar to the ones after each consecutive split. Each following day, the iPS cell colonies grew larger and the iPS cells displayed a compacted and triangular morphology typical for iPS cells. Ideally, in order to keep the iPS cells healthy and undifferentiated, the split into a new plate was performed when the cells reach a confluency of around 70-80%. Cells were usually split every six days. Since the patient-derived iPS cells were not at this stage yet, we show the iPS cell colony growth in another cell line (kiPS3F7) (**Figure 9**).

## 3.4 Characterisation of the SP11.1 iPS cell line

### 3.4.1 Alkaline phosphatase staining

Pluripotent stem cells show expression of alkaline phosphatase and this marker can be used in combination with other markers to verify the pluripotency state. After performing the staining in a plate of SP11.1 iPS cells, clear colonies were observed that were fully stained (**Figure 10**). Hence, this staining is a first indication of pluripotency of this cell line.

### 3.4.2 Transgene silencing

In order for iPS cell to be pluripotent, it needs to be shown that the introduced transgenes are silenced while endogenous pluripotency genes are activated. It is important that the expression of the Yamanaka factors remains between certain ranges [11]. Deviating quantities of the Yamanaka factors result in differentiation of iPS cells. It has been speculated that an overexpression of the Yamanaka factors acts inhibitory on mitosis [11]. Therefore, it is generally considered optimal that only endogenous pluripotency genes should be expressed, while the transgene Yamanaka factors should ideally be silenced. The SP11.1 iPS cell line was retrovirally reprogrammed with only three Yamanaka factors, i.e. *Oct4*, *Sox2* and *Klf4*. After performing an RT-PCR and normalising obtained values with GAPDH expression, a clear silencing of the transgenes (transKlf4, transOct4 and transSox2) were observed (**Figure 11**). Simultaneously, the endogenous expression of Klf4, hOct4 and hSox2 was prominently present. To verify the pluripotent state, expressions of other pluripotency markers were measured as well. Expression of *CRIPTO*, *Nanog* and *Rex1* were clearly elevated and indicate pluripotency of the SP11.1 iPS cell line.

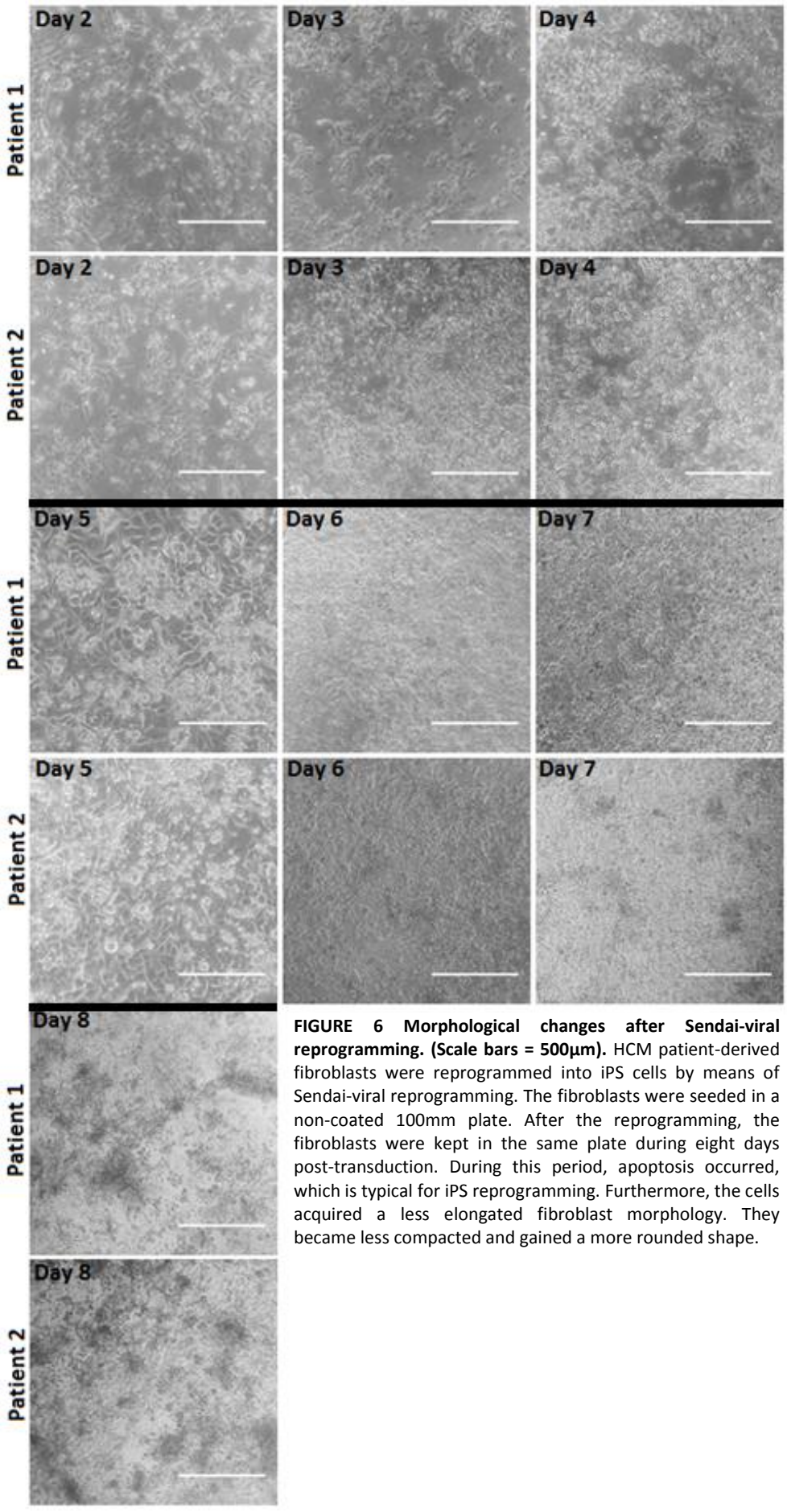


**FIGURE 6 Morphological changes after Sendai-viral reprogramming. (Scale bars = 500µm).** HCM patient-derived fibroblasts were reprogrammed into iPS cells by means of Sendai-viral reprogramming. The fibroblasts were seeded in a non-coated 100mm plate. After the reprogramming, the fibroblasts were kept in the same plate during eight days post-transduction. During this period, apoptosis occurred, which is typical for iPS reprogramming. Furthermore, the cells acquired a less elongated fibroblast morphology. They became less compacted and gained a more rounded shape.

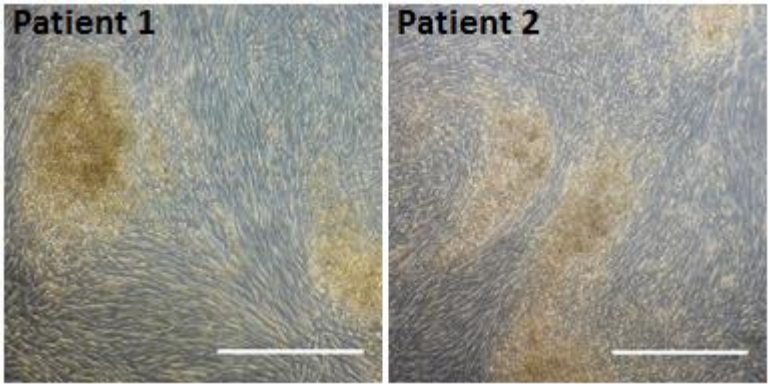


**FIGURE 7 Colony-like structures of partially reprogrammed fibroblasts (Scale bar = 500µm).** One week after reseeding on top of HFF feeders, clusters were observed of small, round, loose and apoptotic cells. These are a normal by-product of iPS cell reprogramming.

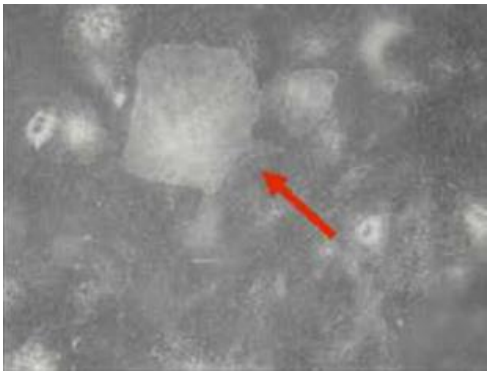

**FIGURE 8 Appearance of iPS colonies.** True iPS cell colonies should appear between two and four weeks of culturing after reseeding on top of feeders. IPS cell colonies typically display angular shapes with the composing iPS cells being compacted and triangular in shape.

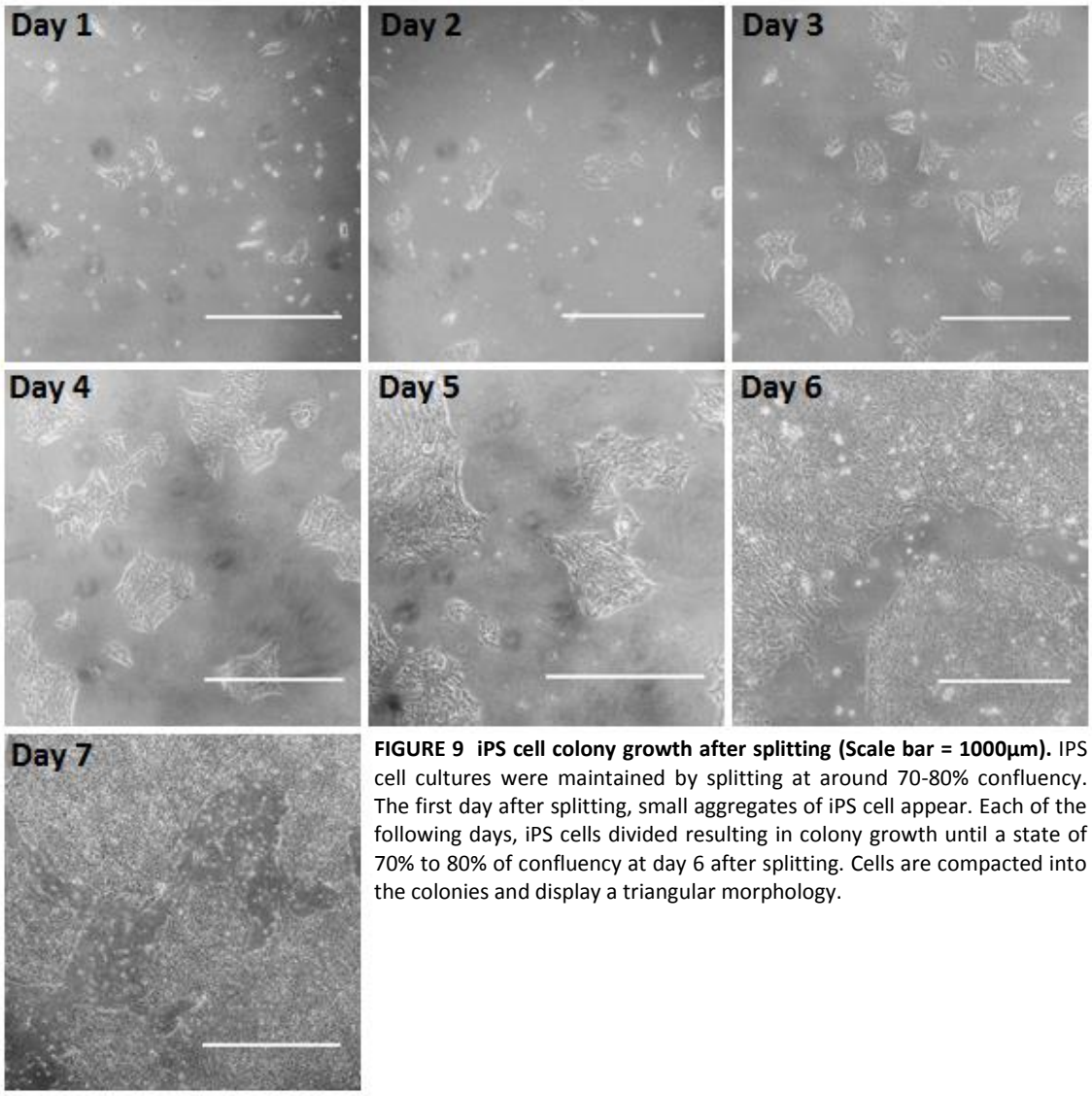


**FIGURE 9 iPS cell colony growth after splitting (Scale bar = 1000µm).** IPS cell cultures were maintained by splitting at around 70-80% confluency. The first day after splitting, small aggregates of iPS cell appear. Each of the following days, iPS cells divided resulting in colony growth until a state of 70% to 80% of confluency at day 6 after splitting. Cells are compacted into the colonies and display a triangular morphology.

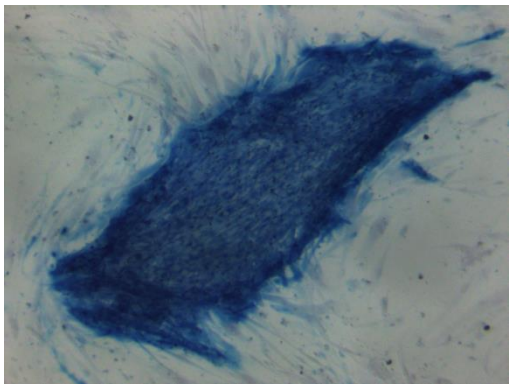

**FIGURE 10 Alkaline phosphatase staining of an iPS cell colony.** Pluripotent stem cells express alkaline phosphatase, which is the target of this staining. Colonies were strongly stained, with a more dense colour in the colony periphery.

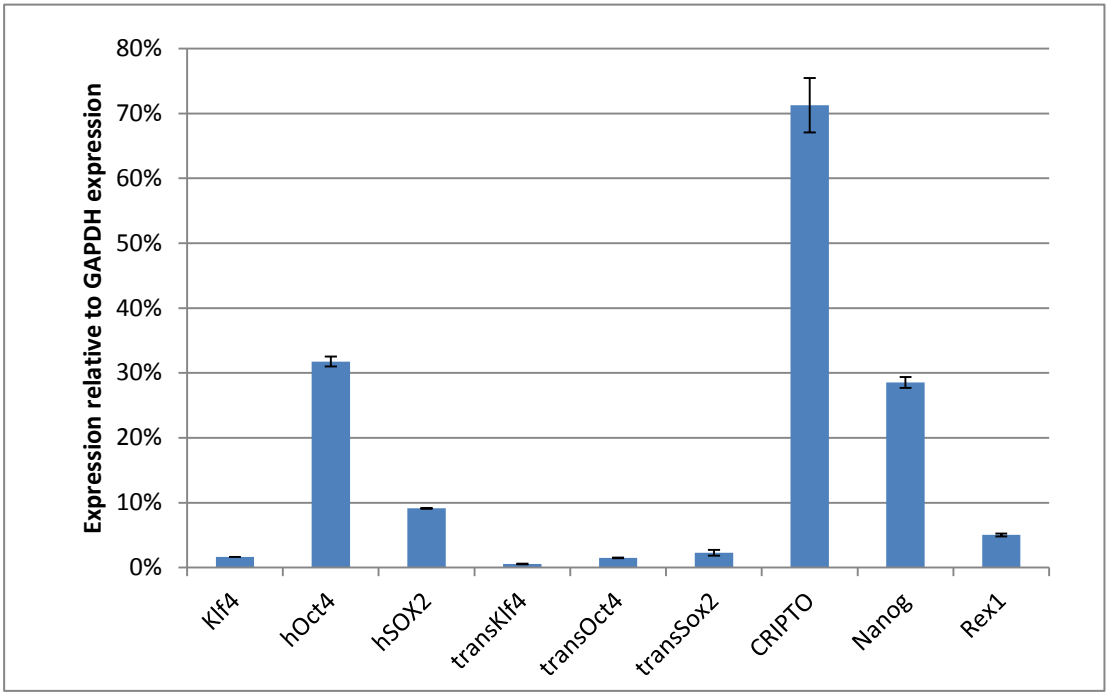


**FIGURE 11 RT-PCR of endogenous and transgene factors.** The transgenes (transKlf4, transOct4 and transSox2) were clearly silenced, while endogenous expression of these factors was prominent. As positive controls, the expression of CRIPTO, Nanog and Rex1 were measured. These pluripotency markers were clearly expressed as well.

### 3.4.3 Karyotype of SP11.1 iPS cell line

In order to be able to use this cell line as a valid control, the genome of the control cell line needs to be void of alterations, translocations, duplications, deletions, and other aberrations. Such deviations in the genome may bias experiments. The external laboratory that performed the karyotyping of this cell line reported that the genome of the SP11.1 cell line has no such deviations (**Figure 12**).

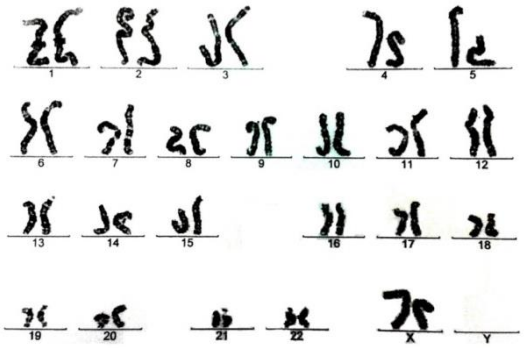

**FIGURE 12 Karyogram of the SP11.1 cell line** The karyogram from the SP11.1 iPS cell line displays a 46,XX genome from a healthy female donor. No alterations in the genome were observed.

### 3.4.4 Pluripotency markers

Pluripotency was also shown by performing immunostaining for common pluripotency markers (**Figure 13**). Nuclear pluripotency markers for this staining were *Nanog*, *Oct4* and *Sox2*. Expression of these markers was visible as green fluorescence, but coincides in Figure 13 with the DAPI staining. Expression of the surface markers Tra-1-81, SSEA-3 and SSEA-4 was most noticeably visible as red fluorescence. The centres of the colonies generally show less expression of pluripotency markers since inner iPS cells are more prone to differentiation and thus are more likely to lose pluripotency.

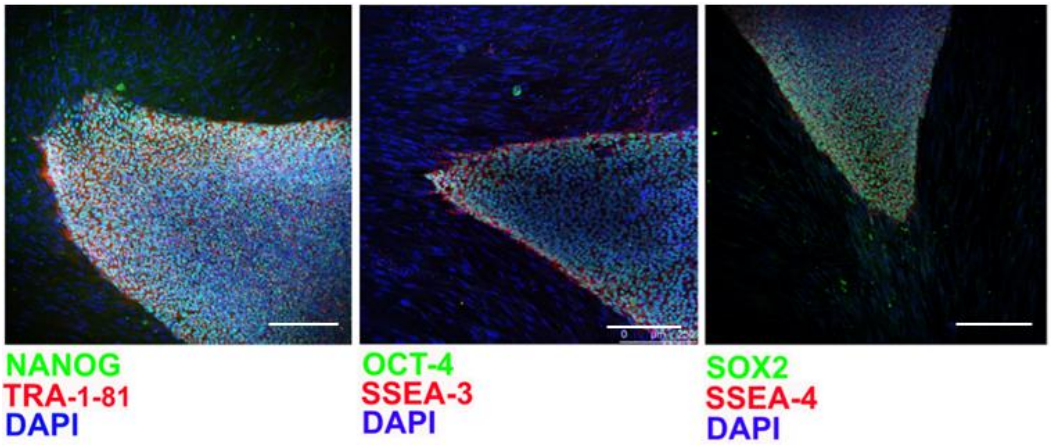


**FIGURE 13 Staining of pluripotency markers.** IPS cell colonies were stained for the nuclear pluripotency markers Nanog, Oct4 and Sox2. Surface pluripotency markers were stained as well, i.e. Tra-1-81, SSEA-3 and SSEA-4. Pluripotency markers were most visible in the edges of the iPS cell colonies. This is due to the fact that the centre of an iPS cell colony is more prone to differentiation. Additionally, nuclei were stained with DAPI.

### 3.4.5 In vitro differentiation of embryoid bodies

EBs were obtained and cultured in differentiation condition for each germ layers. Subsequently, an immunostaining was performed for AFP and FOXA2 in endodermal cells, SMA in mesodermal cells and Tuj1 in ectodermal cells (**Figure 14**). AFP and FOXA2 were abundantly expressed in cells from the endodermal lineage. These endodermal cells displayed a cubical shape. In cells from the mesodermal lineage, SMA was clearly visible and displayed spindle-like shapes. Ectodermal cells which were stained with *Tuj1* revealed clusters of cells with axon-like protrusions. These stainings show that the SP11.1 is truly pluripotent, since it is able to differentiate into each of the three germ layers.

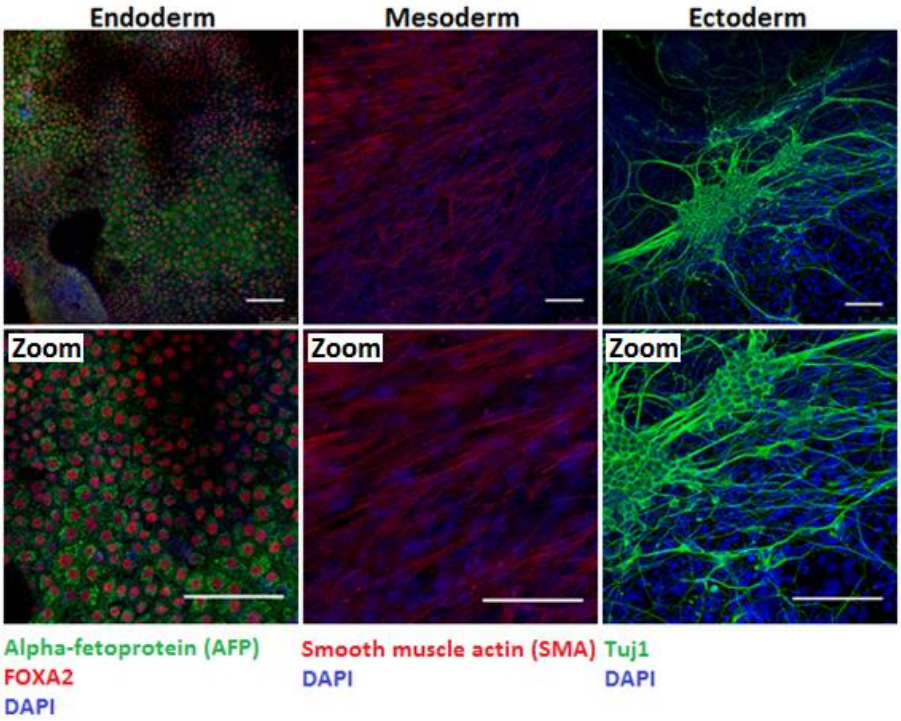


**FIGURE 14 In vitro differentiation into the three germ layers (Scale bars = 100µm).** Endodermal cells were stained for AFP and FOXA2, which was clearly observed. Mesodermal cells showed expression of SMA which revealed spindle-like shapes. Ectodermal cells were stained for Tuj1 and displayed axon-like protrusions.

### 3.4.6 DNA methylation

By means of bisulphite conversion, the unmethylated cytosines were replaced with uracil. The methylated cytosines however were not replaced (**Figure 15**). The five CpG islands of the Oct4 promotors of all clones were demethylated, as well as most of the five CpG islands of the Nanog promotor. Demethylated Nanog and Oct4 promotors are characteristic markers for pluripotency [29]. Hence, the SP11.1 iPS cell line showed a pluripotent state based on these markers.

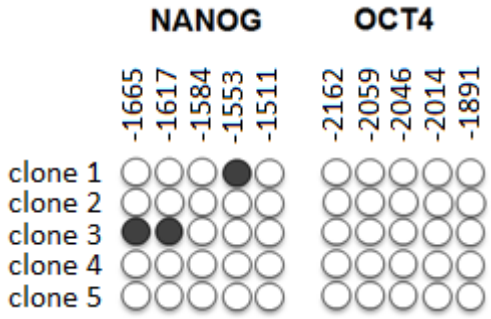


**FIGURE 15 DNA methylation assay of the SP11.1 cell line.** The black-filled balls represent methylated cytosines, while the white balls represent demethylated cytosines. Cytosines of the five CpG-islands of the Nanog and Oct4 promotors were considered. Positions were referred to as relative to the start of the respective gene locus.

### 3.4.7 Teratoma assay

IPS cells were injected in the testes of SCID mice and developed into teratomas. Removed teratomas were stained for endodermal, mesodermal and ectodermal markers (**Figure 16**). In all germ layers staining of the respective markers was observed. These results show that the SP11.1 iPS cell line is indeed truly pluripotent. However, teratoma assays are no longer necessary requirements for the characterisation of iPS cells. In vitro differentiation in combination with the other previous characterisation methods is sufficient to characterise an iPS cell line.

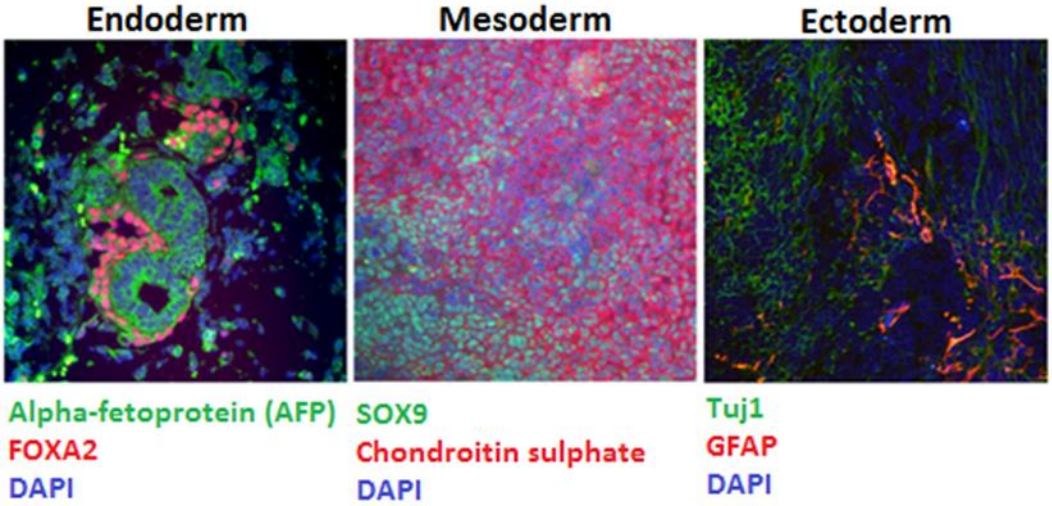


**FIGURE 16 Immunostaining of obtained teratomas.** Endodermal cells were stained for AFP and FOXA2. Mesodermal cells were stained for Sox9 and chondroitin sulphate and ectodermal cells were stained for Tuj1 and GFAP. All cells were additionally stained with DAPI. Endodermal, mesodermal and ectodermal markers were clearly expressed in the teratoma samples. These stainings provide evidence that the iPS cells are capable of committing to all three germ layers.

## 3.5 PCR and gel electrophoresis of the constructs

In order to amplify and purify all sequences for the constructs, a PCR was needed. After the PCR, the PCR fragments were used to ligate into the pcDNA3 vector, which was amplified in an *Escherichia Coli* culture. Before PCR amplification of the actin and RFP sequences, PCR primers needed to be designed for both constructs containing these sequences. Since the aim was to use the HindIII restriction site in the pcDNA3 vector, the first sequence to be inserted needed to have such a restriction site as well. The two sequences were linked with by using a BamHI restriction site and a linker sequence ACTAGTGGC. For the RFP-actin construct, the forward primer of RFP was 5'-aa**AAGCTT**ATGGCCTCCTCCGAGGACG-3'. The first two adenosines act as a buffer for degradation of the primer. AAGCTT is the HindIII restriction site, which is followed by the first 19 nucleotides of the first exon of the RFP sequence. The reverse primer for RFP was 5'-aa**GGATCC**~~TTA~~GGCGCCGGTGGAGTGG-3'. In this reverse primer the first two adenosines were followed by the BamHI restriction site GGATCC and subsequently by the reverse complement of the 16 last coding nucleotides of RFP. One should note that the reverse complement TTA of the stop codon should not be included in the primer. If not, this will cause the fusion protein construct to have a premature stop codon. The forward primer for sarcomeric actin was 5'-aa**GGATCC***ACTAGTGGC*ATGTG TGACGACGAGGAGAC-3'. The first two

adenosines were followed by the BamHI restriction site GGATCC, by the linker sequence ACTAGTGGC, and by the 20 first coding nucleotides of sarcomeric actin. The reverse primer for sarcomeric actin was 5'-aa**GAATCC** TTAGAAGCATTTGCGGTGGAC-3', in which GAATCC is the restriction site of EcoRI. The restriction site was followed by the 21 last coding nucleotides of sarcomeric actin. In contrast to the reverse primer of RFP, here the stop codon is included since this sarcomeric actin sequence is the last coding part of the designed RFP-actin fusion protein.
Analogously, the PCR primers for the actin-RFP construct were designed in a similar manner. The same restriction sites and linker sequence were used. The forward primer for sarcomeric actin for this construct was 5'-aa**AAGCTT**ATGTGTGACGACGAGGAGAC-3' and the reverse primer was 5'-aa**GGATCC**TTAGAAGCATTTGCGGTGGAC-3'. The forward primer for RFP for the actin-RFP construct was 5'-aa**GGATCC***ACTAGTGGC*ATGGCC TCCTCCGAGGACG-3'. The reverse primer for this construct was 5'-aa**GAATCC**TTAGGCGCCGGTGGAGTGG-3'.

Similarly, the PCR primers for the MYBPC3 constructs were designed. However, for the these constructs the KpnI restriction site was used instead of the HindIII restriction site, since the MYBPC3 sequence itself contains a HindIII restriction site. For the MYBPC3-GFP construct, the forward primer for MYBPC3 was 5'-aa**GGTACC**ATGCCTGAGCCGGGGAAGAA-3'. The reverse primer for MYBPC3 was 5'-aa**GGATCC**~~TGA~~CTGAGGCACTCGCACCTCC-3'. The forward primer for GFP was 5'-aa**GGATCC***ACTAGTGGC*ATGGTGAGCAAGGGCGAG-3' and the reverse primer for GFP was 5'-aa**GAATTC**TTACTTGTACAGCTCGTCC-3'. For the GFP-MYBPC3 construct, the forward primer for GFP was 5'-aa**GGTACC**ATGGTGAGCAAGGGCGAG-3' and the reverse primer was 5'-aa**GGATCC**~~TTA~~CTTGTACAGCTCGTCCA-3'. The forward primer for MYBPC3 was 5'-aa**GGATCC***ACTAGTGGC*ATGCCTGAGCCGGGGAAGAA-3' and the reverse primer was 5'-aa**GAATTC**TCACTGAGGCACTCGCACCT-3'.
After design and ordering of the PCR primers , the PCR was performed as well as a subsequent gel electrophoresis to verify the presence and size of the sequences of actin and RFP (**Figure 16**). The MYBPC3 constructs were created before the start of this project. The size of the PCR fragments was upfront calculated by means of the Serial Cloner and SnapGene software. The PCR confirmed the calculated sizes of the PCR fragments.

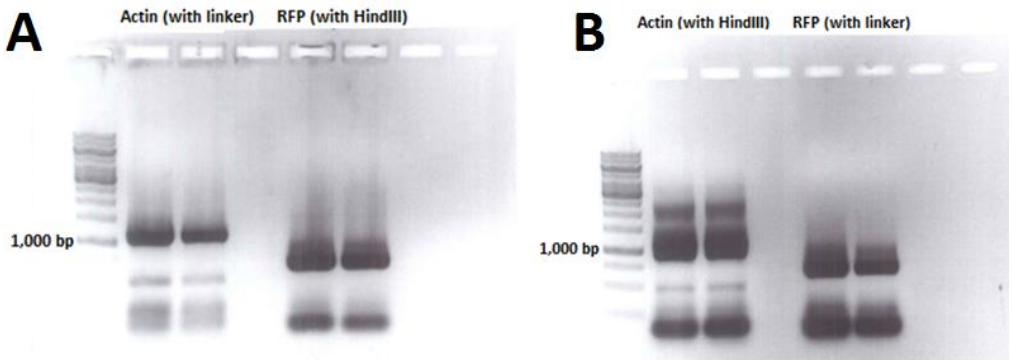


**FIGURE 16 Gel electrophoresis of PCR-derived RFP-actin sequences (Panel A) and PCR-derived actin-RFP sequences (Panel B).** The initial actin and RFP sequences for the RFP-actin construct had a length of 1159 and 694 nucleotides respectively. The actin and RFP sequences for the actin-RFP construct had a length of 1145 and 703 nucleotides respectively. A gel electrophoresis of the PCR-derived sequences confirmed these sequence sizes as well as their proper amplification. The gel also allowed to purify the sequences by cutting them out and resolubilising them.

## 3.6 Testing of vector transfection efficiency

In order to test whether the ACTC1 and MYBPC3 fusion genes are translated properly, they were first transfected into 293T cells and HEK293 cells respectively. After transfection with the respective constructs and start of selection, fluorescence was measured every two days (**Figure 17-19**). Gradually increasing differences were observed between the three concentrations with which the 293T cells were transfected. On the sixth day after puromycin selection, the majority of the 293T cells that were transfected with 2.50µg/ml and 3.75µl/ml of either construct died. Only the 293T cells that were transfected with 1.25µl/ml had a fairly good survival. Therefore, for both the ACTC1-RFP construct and RFP-ACTC1 construct, the optimal concentration for transfection into 293T cells is 1.25µl/ml. The transfection of the HEK293 cells with the MYBPC3 constructs was performed later and hence those results were not available yet.

## 3.7 Maps of designed constructs

By means of the SnapGene software, the sequences of ACTC1 cDNA, MYBPC3 cDNA, RFP, and the pcDNA3 vector were used to draw maps of the constructs that were designed. As the MYBPC3 sequence contains a HindIII restriction site, the first restriction site used was the KpnI restriction site in the multiple cloning site (MCS) of the pcDNA3 vector. For the MYBPC3-GFP construct and the GFP-MYBPC3, the KpnI restriction enzyme was thus used, as well as the BamHI and EcoRI enzymes. With this information and the sequences available, maps were drawn for the MYBPC3-GFP (**Figure 20**) and GFP-MYBPC3 constructs (**Figure 21**).
For the ACTC1-RFP (**Figure 22**) and RFP-ACTC1 (**Figure 23**) constructs the HindIII, BamHI and EcoRI restriction sites were used to integrate the PCR fragments in the pcDNA3 vector. SnapGene was used as well to draw maps for the ACTC1 constructs. Important for selection purposes was the replacement of the neomycin resistance cassette by another antibiotic resistance cassette. This allows selecting cells for presence of both an ACTC1 and a MYBPC3 construct. In order to do this, the puromycin cassette was removed by cleaving and blunting the Sma1 and Bsm1 restriction sites. The puromycin was removed of its commercial vector by cleaving and blunting the HindIII and BamHI restriction sites. Subsequently, the puromycin cassette was put inside the pcDNA3 vector.

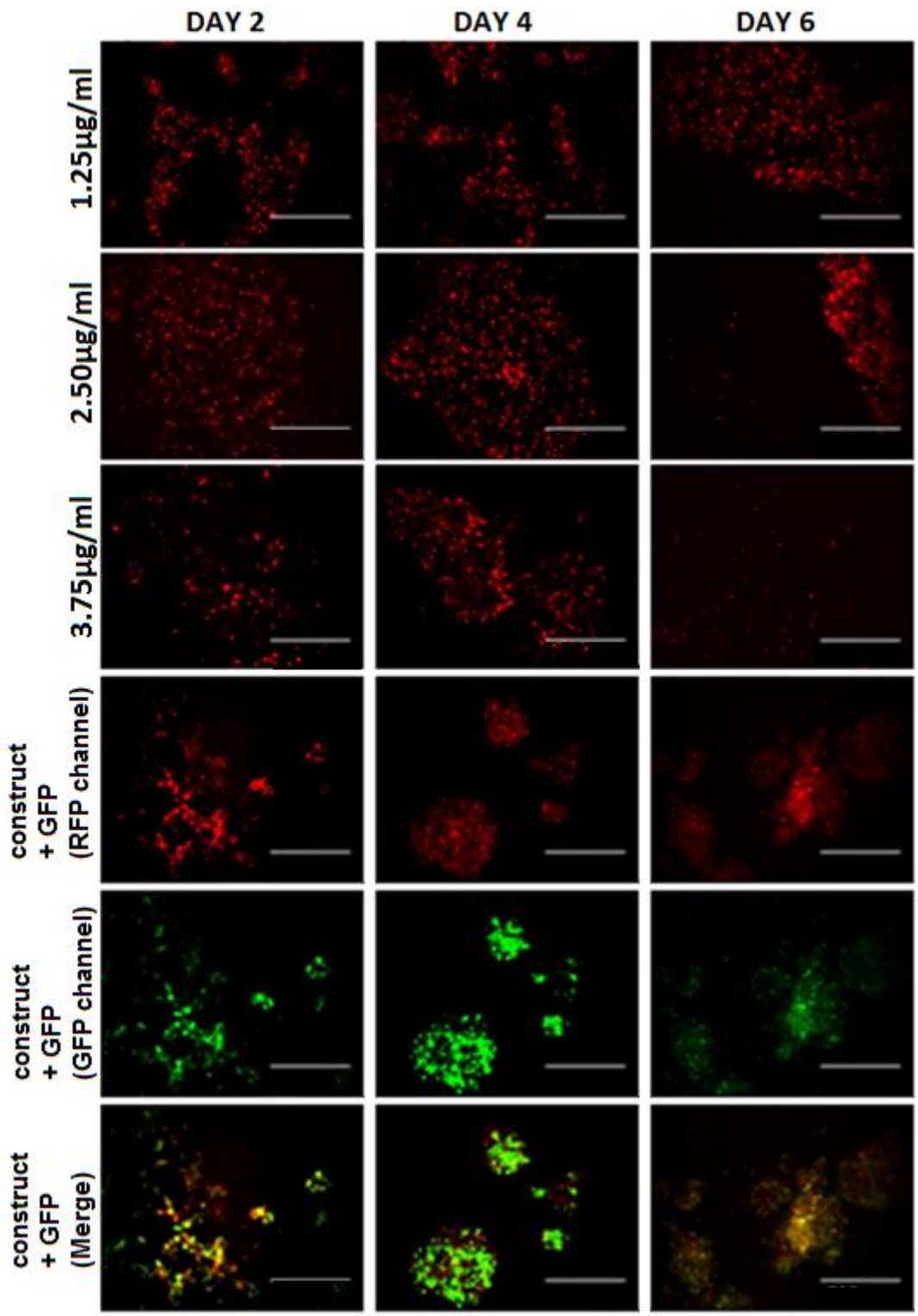


**FIGURE 17 Testing of the ACTC1-RFP construct in 293T cells (Scale bars = 500µm).** Three different transfection concentrations of the ACTC1-RFP construct were assessed. At a concentration of 2.50µg/ml and 3.75µg/ml, cell apoptosis of the transfected cells was observed. Only a concentration of maximum 1.25µg/ml allowed survival of transfected cells during puromycin selection. A double transfection with a GFP vector was included, as a positive control for the designed construct. In case no signal of RFP would have been observed but in presence of a GFP signal, this would indicate a defect in the function or design of the construct.

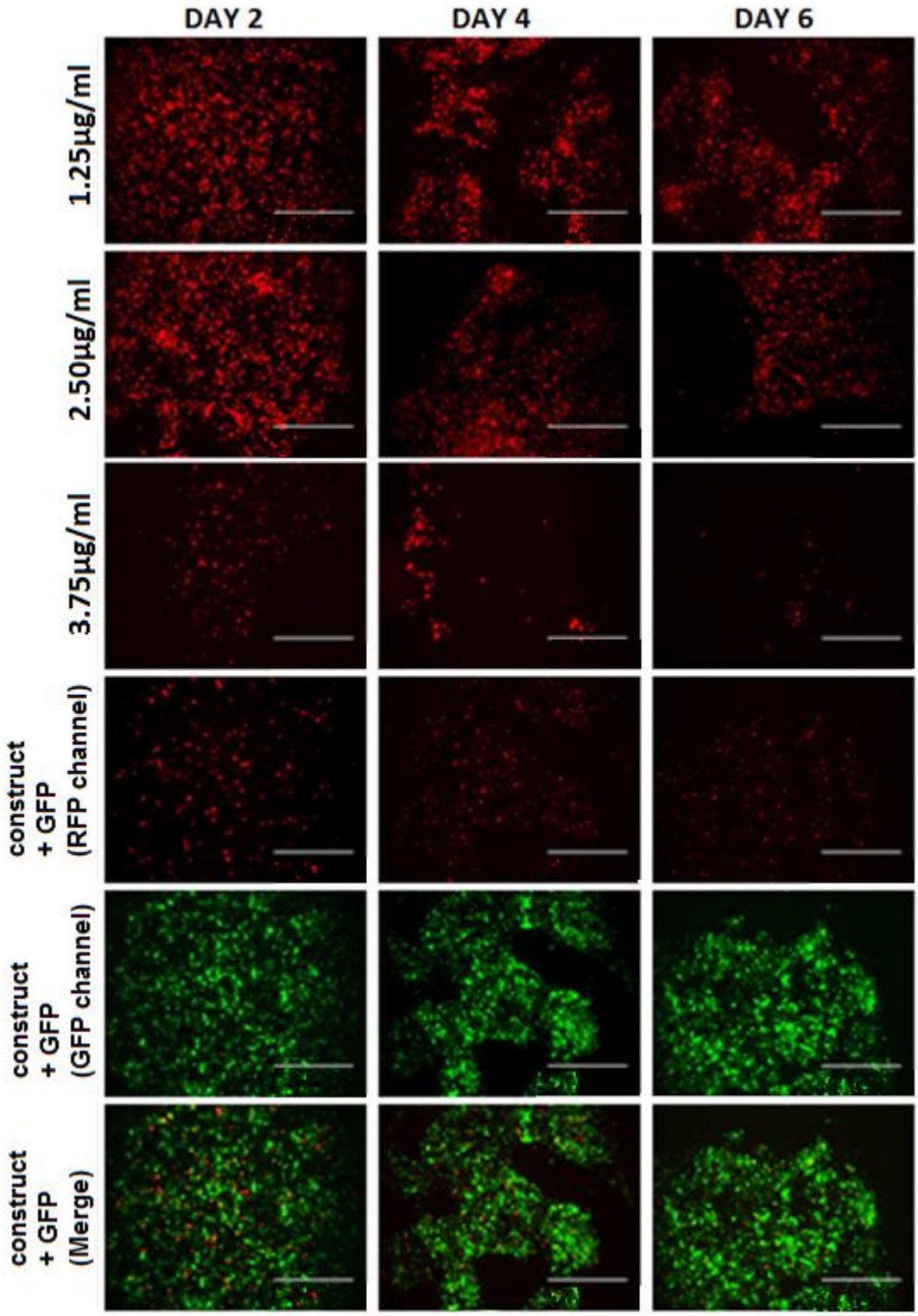


**FIGURE 18 Testing of the RFP-ACTC1 construct in 293T cells (Scale bar = 500µm).** Three transfection concentration of ths construct were tried as well. Results were similar to those of the ACTC1-RFP construct, i.e. concentrations of 2.5µg/ml and 3.75µg/ml were detrimental for most of the cells. A maximum concentration of 1.25µg/ml allowed sufficient cell survival during puromycin selection. A double transfection control was included as well for the testing of the RFP-ACTC1 construct.

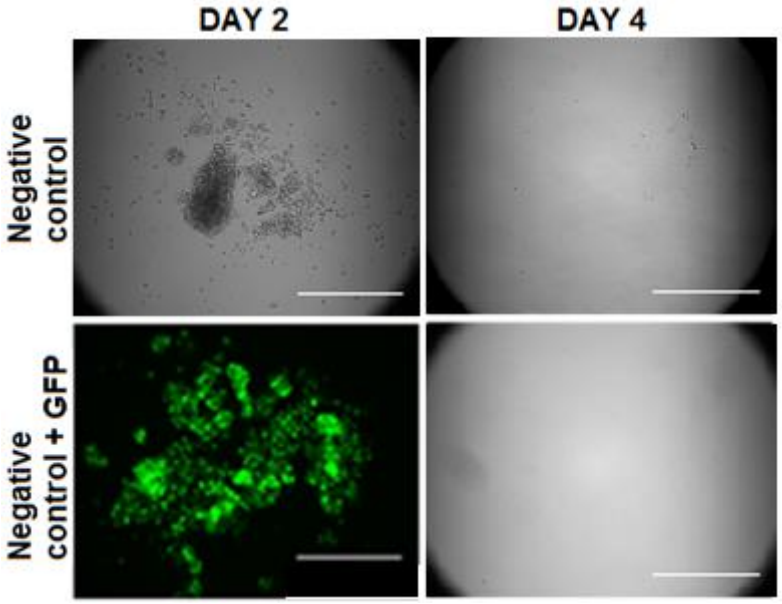


**FIGURE 19 Controls of the 293T cell transfections with the ACTC1 constructs (Scale bars = 500µm).** A blank control and a control transfected with only a GFP vector were included. For both controls, substantial apoptosis was observed two days after puromycin selection. Four days after selection, none of the cells of either control group survived.

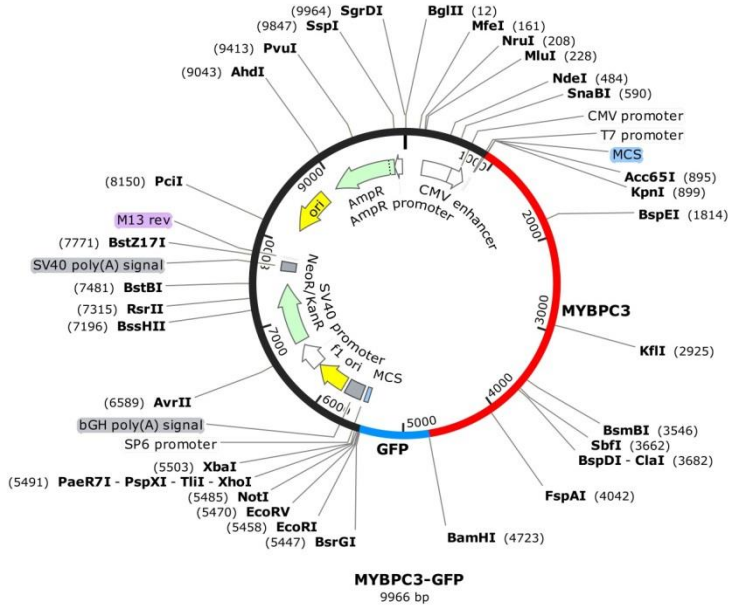


**FIGURE 20 MYBPC3-GFP construct with a neomycin resistance cassette.** The KpnI, BamHI and EcoRI restriction enzymes were used to integrate the two PCR fragments into the pcDNA3 vector. The original neomycin/kanamycin resistance cassette was kept in the vector.

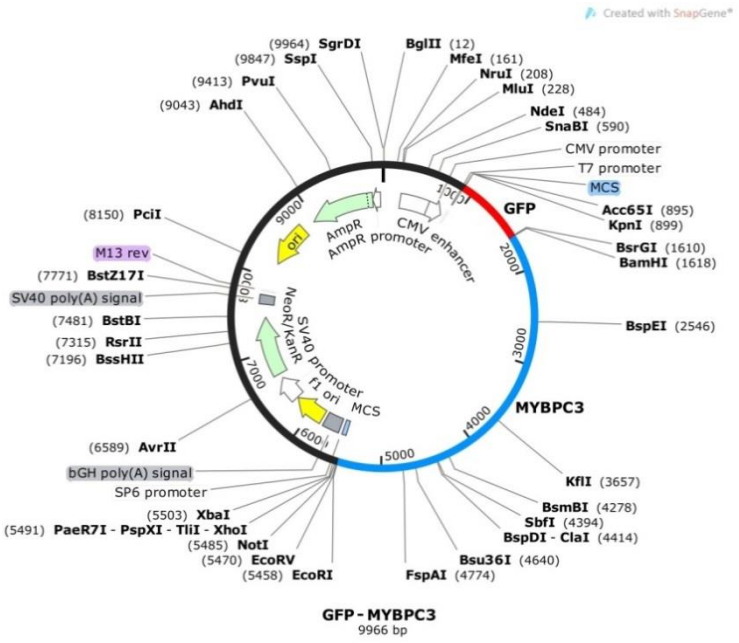


**FIGURE 21 GFP-MYBPC3 construct with a neomycin resistance cassette.** The KpnI, BamHI and EcoRI restriction sites were used to ligate the two PCR fragments into the pcDNA3 vector. The original antibiotic resistance cassette was kept in the vector.

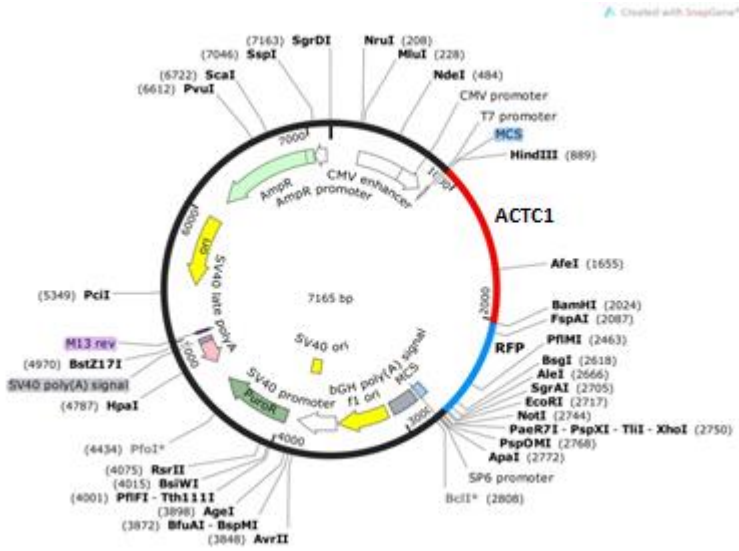


**FIGURE 22 ACTC1-RFP construct with a puromycin resistance cassette.** The HindIII, BamHI, and EcoRI restriction sites were used for the ligation of the PCR fragments into the pcDNA3 vector. The neomycin resistance cassette was removed by cleaving and blunting of the Sma1 and Bsm1 restriction sites. Subsequently, the puromycin resistance cassette was removed out of its commercial vector by cleaving and blunting with HindIII and BamHI. The blunted vector and blunted puromycin resistance cassette were then ligated.

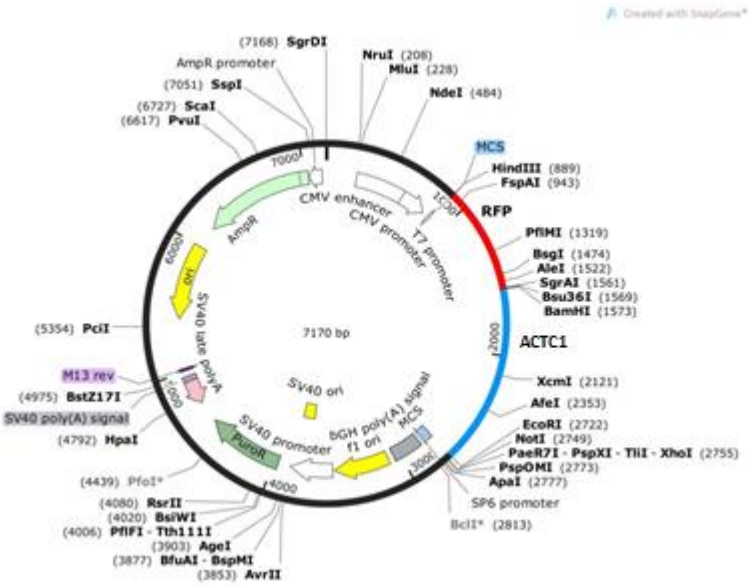


**FIGURE 23 RFP-ACTC1 construct with a puromycin resistance cassette.** The HindIII, BamHI, and EcoRI restriction sites were used to insert both PCR fragments into the pcDNA3 vector. Additionally, also the neomycin resistance cassette of this vector was replaced by a puromycin resistance cassette, analogously to the replacement in the ACTC1-RFP construct.

## 3.8 Cardiomyocyte differentiation by the GiWi protocol

By means of the GiWi protocol described by Lian et al. (2013) [17], iPS cells differentiated into functional, i.e. beating, cardiomyocytes. As is normal for this protocol, cell death was observed during the first days after start of the protocol (**Figure 25**). As of nine days after start of differentiation, a gradually increasing formation of a cardiomyocyte mesh was observed. Cells were growing in clusters, which grew connected one to the other by cardiomyocyte strings. Cardiomyocytes in these strings started contracting as of day 11. The axis of contraction was longitudinally oriented in the strings. After several days longer of culturing, some of the wells of the plates showed the development of a synchronously beating layer of cardiomyocytes. These layers typically had one to four regions where pulses initiated, indicating multiple 'pacemaker' regions.

## 3.9 IPS cell-derived cardiomyocyte immunostaining

IPS cell-derived cardiomyocytes were stained for Troponin I, cMyBP-C and DAPI. The immunostaining clearly displayed the sarcomeric filaments by both the staining of Troponin I and cMyBP-C (**Figure 26**). However, Troponin I staining was only present in the I-bands of the sarcomeres, while cMyBP-C staining typically occurred in the A-bands. This alternating and complementary staining of the sarcomeres was clearly observed in these cardiomyocytes (**Figure 26 Zoom D**). Hence, a proper function of the newly purchased cMyBP-C antibody was shown.

## 3.10 CRISPR-Cas9 genome editing

The efficiencies of the gRNA candidates were first tested in a T7E1 assay. The efficiencies for gRNA1, gRNA2, and gRNA3 were respectively 5.28%, 3.92% and 6.24%. Hence, the gRNA3 sequence was used for the transfection of the SP11.1 iPS cell line. The SP11.1 iPS cell line was transfected with the Cas9 enzyme, the *Nkx2.5*-RFP donor and the selected gRNA. Selection with both geneticin (positive selection) and ganciclovir (negative selection by thymidine kinase/ganciclovir) was started, after which substantial apoptosis was observed (**Figure 24**). However, survival of a subset of iPS cell indicated antibiotic resistance and hence successful transfection. The morphology changed from typical iPS cell features to more cubical or triangular cell shapes. Cells were also disaggregated from each other, so that iPS cells were not organised any longer in iPS cell colonies.

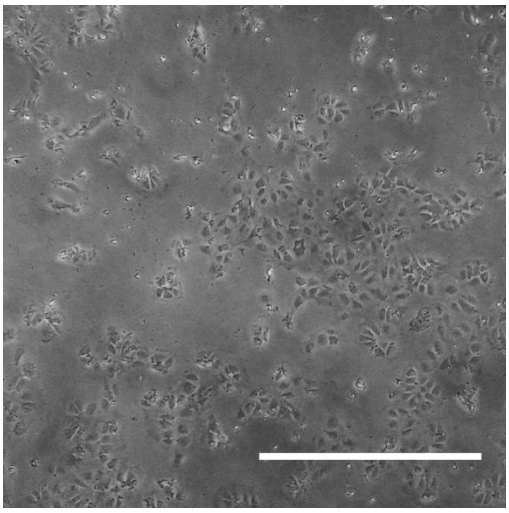

**FIGURE 24 CRISPR-Cas9 transfection of SP11.1 iPS cells with the Nkx2.5-RFP construct. (Scale = 500µm)** After selection, apoptosis was observed and surviving cells no longer appeared in colonies. Cells became more angular in shape.

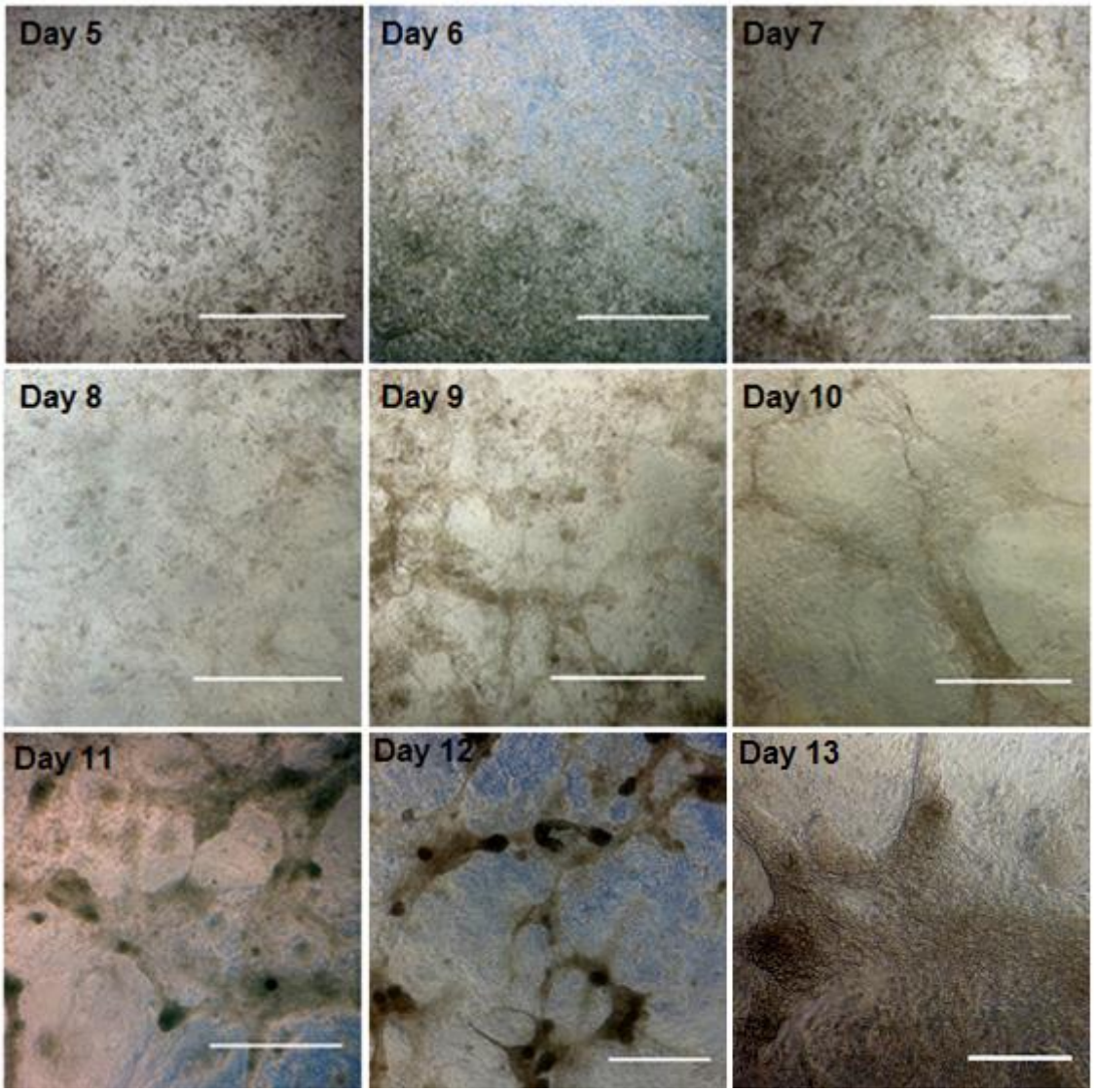


**FIGURE 25 Cardiomyocyte differentiation by the GiWi protocol (Scale bar = 500µm).** The first days after seeding iPS cells and starting the GiWi protocol, a substantial amount cell death was observed. Up to day 8, mainly small clusters of dead cells were floating in the medium. As of day 9, cardiomyocyte meshes were gradually formed. These meshes consisted of cell aggregates interconnected with cardiomyocyte strings. Cardiomyocyte strings started contracting as of day 11. In several wells of the differentiation plate, a gradual synchronisation of beating was observed (Day 13).

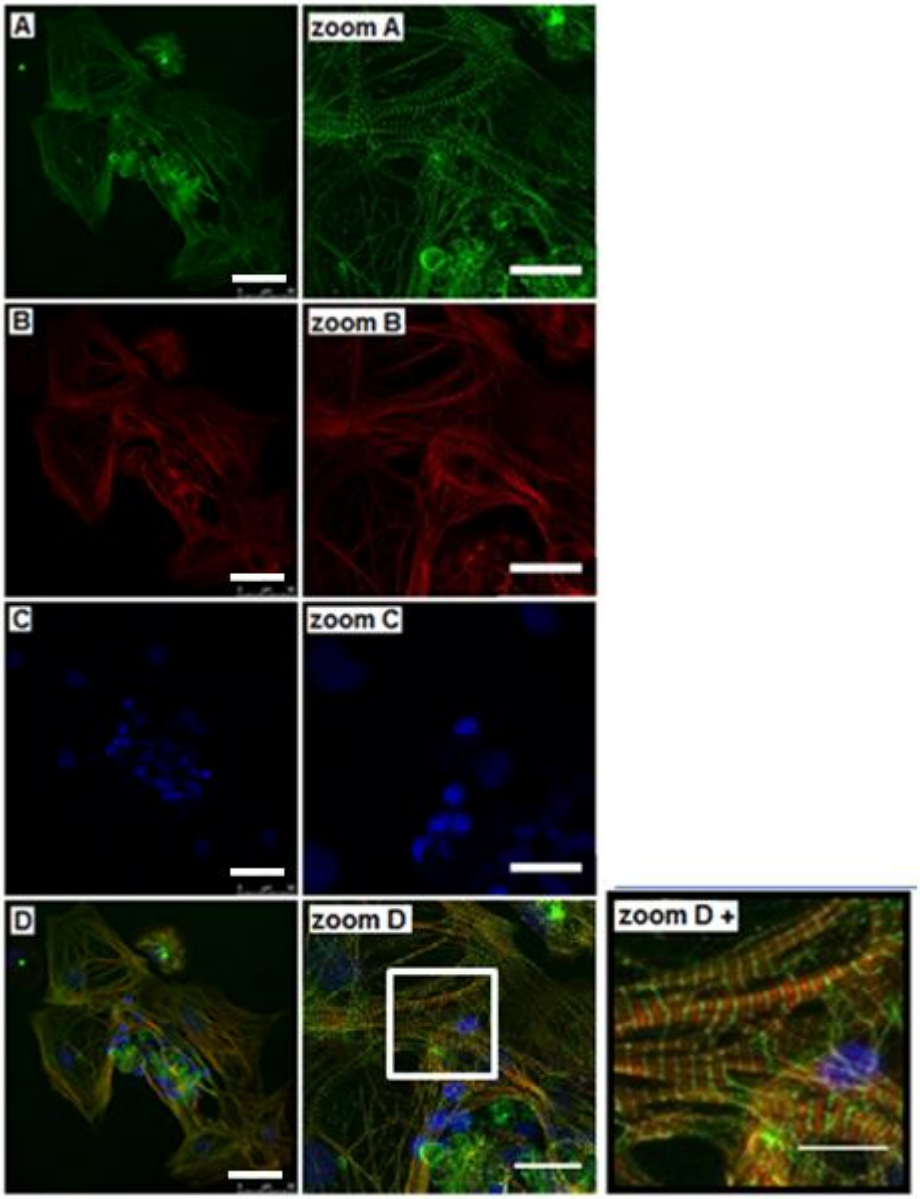


**FIGURE 26 IPS cell-derived cardiomyocyte immunostaining. A**. Staining of cMyBP-C. **B**. Staining of Troponin I. **C**. DAPI staining of the nuclei. **D**. Merge. CMyBP-C and troponin I stainings revealed complementary staining of sarcomeres (Zoom D). The I-bands were stained with the Troponin I antibody and the A-bands were stained with the cMyBP-C antibody. (Scale bars A, B, C and D = 50µm ; Scale bars Zoom A, B, C and D = 25µm ; Scale bar Zoom D+ = 15µm)

# 4. Discussion

## 4.1 Construct design

When designing fusion protein labels, often the first two fusions considered are C-terminal fusing and N-terminal fusing. This is due to the fact that the C-terminus and N-terminus are usually situated on the protein surface and hence the fused labels (GFP and RFP) are less likely to interfere with protein folding and functionality. However, in the context of studying actin-cMyBP-C interactions, it is possible that a relatively large protein such as GFP or RFP causes sterical hindrances. It will be investigated with Förster Resonance Energy Transfer (FRET) and dynamic cell traction force microscopy whether there is one of the four constructs combinations where no such sterical hindrance exists. Should all of the construct combinations interfere with the actin-cMyBP-C interactions, labels will need to be designed that target other protein regions.
Furthermore, in the future it might prove beneficial to insert the fusion gene constructs into the genome of iPS cells by a targeted approach such as CRISPR-Cas9 or TALEN technology. With our constructs, fusion proteins that are randomly inserted into the genome might be altering cell functions. Even more, the cells will express both endogenous and exogenous proteins which might compromise experimental results.

## 4.2 Testing of vector transfection efficiency in 293T cells

After transfecting each of the designed constructs into 293T cells, fluorescence was observed. This shows that the constructs are properly translated and that at least the GFP and the RFP labels function properly. However, it is not known whether the exogenous cMyBP-C and sarcomeric actin is folded properly and functions normally. Once transfected iPS cell are differentiated into cardiomyocytes, the RFP and GFP emissions could be visualised in order to investigate proper sarcomeric integration of the fusion proteins.

## 4.3 Cardiomyocyte differentiation

Cardiomyocyte differentiation protocols still have a relatively low efficiency with significant apoptosis occurring. Furthermore, the surviving cells are a rather heterogeneous group of cardiomyocytes and several other not further determined cell types. Of the cardiomyocytes arising, a wide variety in synchronicity was observed. Contractions often initiated in several regions of the cardiomyocyte mesh. This suggests that gap junction formation and thus synchronicity is not present to the same extent in all derived cardiomyocytes. Furthermore, cardiomyocyte differentiation and maturation might not be ideal in monolayer cultures. In live organisms, cardiomyocytes mature by the presence of an extracellular matrix with a certain Young's modulus. They mature as well by straining and stretching and electrical stimuli. It will prove beneficial to develop new methods that combine all of these factors for a more optimal cardiomyocyte differentiation and maturation.

## 4.4 Future prospects

### 4.4.1 Near future

After transfection of the SP11.1 iPS cells with the constructs in all possible combinations, one of the construct combinations will be selected for further research in both control cell lines and patient-specific iPS cell lines (Figure 27). The construct combination will be selected based on both its signal in Förster Resonance Energy Transfer (FRET) and functional interference in the cardiomyocytes' contractility. Since FRET signals are produced only at small separation distances and since these distances will provide information about actin-cMyBP-C bounds, we will select the construct combination for which the separation distance is the smallest and thus the emission intensity is the highest. However, close proximity of the GFP and RFP labels may cause sterical hindrances that interfere with the actin-cMyBP-C interactions. In order to determine whether such interference occurs, dynamic cell traction force microscopy (dCTFM) will be performed. Hence, taking both results from the FRET and dCTFM together, the best construct combination will cause no interference while still producing a clearly detectable FRET emission signal. In case none of the construct combinations fulfills both criteria, actin and cMyBP-C will need to be labelled in a non-terminal region of the protein. However, it would need to be a region where labelling does not interfere either with the functionality of the protein.

After determining the optimal construct combination and after completion of the patient iPS reprogramming, the resulting iPS cells will be characterised in a similar way as the SP11.1 control iPS cell line. The patient-specific iPS cells will then be transfected with both constructs of the optimal construct combination. Both control cell line and patient-specific iPS cell line will then be differentiated into cardiomyocytes. After differentiation, both groups will be subject to FRET and dCTFM in order to determine differences between healthy controls and HCM cardiomyocytes. However, as mentioned before, HCM mutations are not fully penetrant, indicating other factors are involved in HCM development. Therefore, pathways that influence cMyBP-C will be investigated. Such pathways are the cAMP-dependent PKA pathway, the PKC pathway, the PKD pathway and the CaMKII pathway.

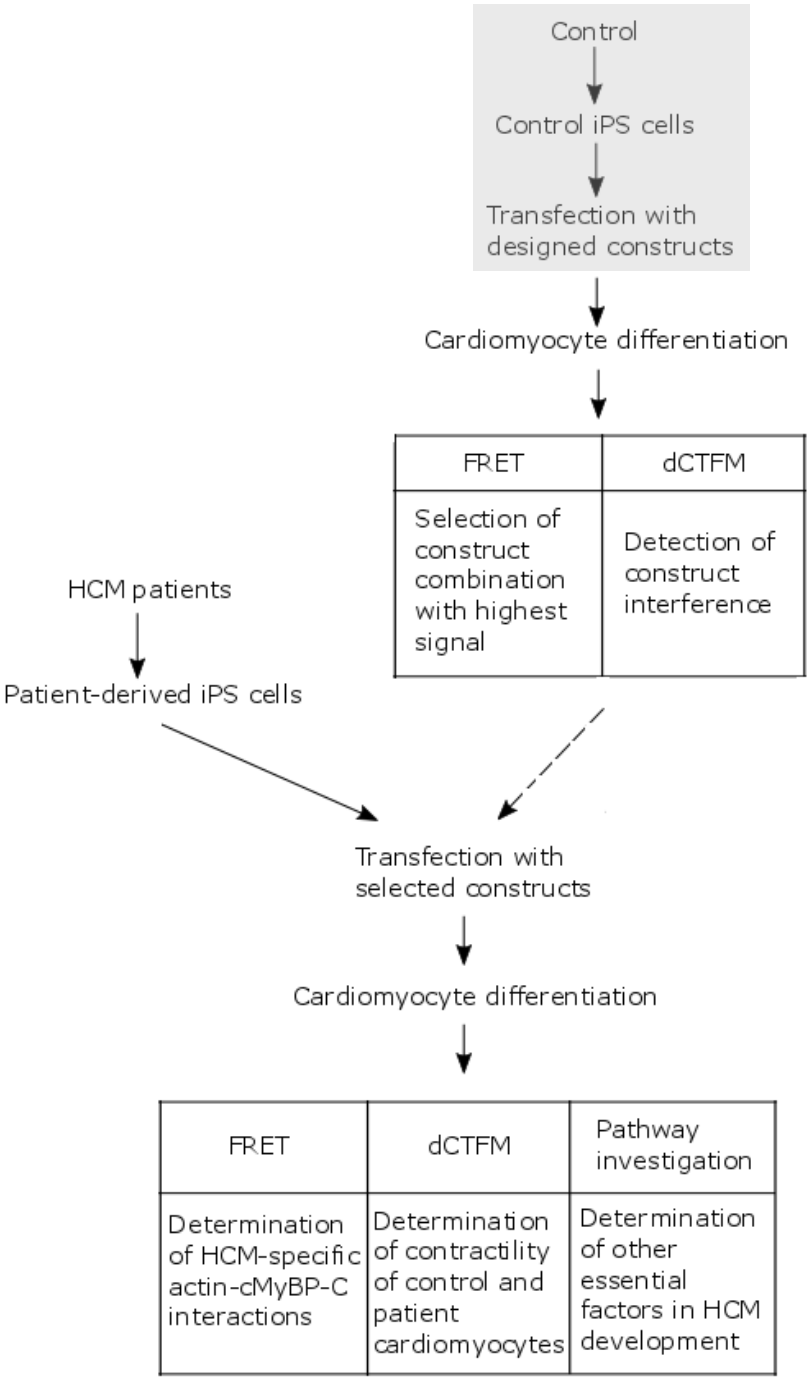


**FIGURE 27 Flow chart of planned research.** Control fibroblast have been differentiated into iPS cells and subsequently transfected with the construct combinations (Grey box). Subsequently , these transfected iPS cells will be selected and differentiated into cardiomyocytes. Cardiomyocytes will then be subject to FRET and dCTFM in order to determine the most optimal construct combination. HCM patient-derived iPS cells will then be transfected with this construct combination. Both control group and HCM patient group transfected with this construct combination will be differentiated into cardiomyocytes. FRET, dCTFM and pathway investigation will provide information about the functional differences between HCM patients and healthy controls regarding actin-cMyBP-C interactions.

### 4.4.2 Förster Resonance Energy Transfer

Förster Resonance Energy Transfer is a theory developed by Theodor Förster [30]. The theory describes the non-radiative energy transfer that occurs between a donor molecule and an acceptor molecule. This energy transfer occurs via Coulombic coupling of the oscillating dipole donor and acceptor molecules [30]. The donor molecule in our system will be the GFP fusion protein, which will be excited by absorbing light with a wavelength of 395nm. The excitation energy causes an outer electron to move into a higher energy state. After the vibrational relaxation of the excited electron, the absorbed energy dissipates into the system. In the absence of an acceptor molecule, this dissipation mainly consists of the emission of a photon with lower energy and thus a higher wavelength. However, also some non-radiative energy dissipation into the medium may occur. In case an acceptor molecule is in close proximity of the donor, energy dissipation from the donor will result in excitation of the acceptor molecule which was in our system RFP. The efficiency of this energy transfer is inversely related to the sixth power of the distance between the centres of the donor and acceptor molecules *r* [30] (Formula 1), where *E* is the efficiency of the energy transfer and $R_0$ is the Förster separation distance.

$$E = \frac{1}{1+\left(\frac{r}{R_0}\right)^6} \qquad (1)$$

The Förster separation distance (Formula 2)[30] is the distance at which FRET efficiency is 50%. $R_0$ is dependent on the quantum yield $\Phi_D^0$ in absence of the RFP acceptor molecule, the dipole orientation factor $\kappa^2$, the refractive index of the surrounding medium *n* and the spectral overlap integral *J* of the donor emission spectrum and the acceptor absorption spectrum. $N_A$ is the number of Avogadro. The dipole orientation factor is defined by the angles between the transition dipole moments of the donor and the acceptor [30,31]. Often a random orientation is assumed which results in $\kappa^2 \approx \frac{2}{3}$.

$$R_0^6 = \frac{9000\,(ln10)\Phi_D^0\,\kappa^2 J}{128\pi^5 n^4 N_A} \qquad (2)$$

The Förster separation distance for the eGFP-mRFP1 FRET pair has been calculated at $4.7 \pm 0.5$ nm [32] with n=1.3 as the water refractive index.

As described before, constructs were designed coding for cMyBP-C-GFP and GFP-cMyBP-c fusion proteins as well as constructs coding for *ACTC1*-RFP and RFP-*ACTC1* fusion proteins. The GFP fusion protein labels will function as the donors for FRET, while the RFP fusion protein labels will function as the FRET acceptors. During the FRET analysis, GFP molecules will be excited with light with a wavelength of 395nm and the subsequent emission intensities of the RFP molecules will be measured. The efficiency will be measured and hence the distance *r* between the donors and acceptors can be calculated with the FRET efficiency formula (Formula 1). This distance is representative for the distance of cMyBP-C with actin. Since in an HCM setting the interaction of cMyBP-C and actin supposedly is disturbed, we thus expect this to be reflected in the FRET measurements. FRET measurements will be obtained for all four construct combinations and subsequently cross-referenced with the cell traction force

measurements. The ideal construct combination is the one that has the highest FRET efficiency and does not affect cardiomyocyte contractility.

### 4.4.3 Dynamic cell traction force microscopy

Whenever a cell is attached to a substrate, it senses the elasticity of this substrate and responds to it by applying a force proportional to this elasticity (**Supplemental figure S8**) [33]. This sensing occurs via the so-called focal adhesions. Focal adhesions are membrane associated protein clusters containing transmembrane integrins that bind to the extracellular matrix or an *in vitro* substrate. Furthermore, several other proteins are coupled to the integrins and communicate substrate elasticity within the cell. Paxillin and talin are integrin-binding proteins that stimulate focal adhesion kinase (FAK) and α-actinin to bind actomyosin filaments to the focal adhesions [34,35]. It has been observed that sarcomeres are most efficiently formed in cardiomyocytes when they are grown on a substrate with a Young's modulus $E \approx 10\ kPa$ [33]. Growing on less stiff substrates decreases the development of sarcomeres while stiffer substrates causes the cardiomyocytes to develop stress fibres and disturbs the alignment of sarcomeres[33]. Developing traction forces in response to substrate elasticity somehow regulates sarcomere formation and alignment. This basal state of cardiomyocyte contraction is a measure for the cell's contractility. In this project, it will be of interest whether the fusion protein constructs affect the contractility. Hence, traction forces of non-transfected cardiomyocytes will be compared to those of each of the four transfected cardiomyocyte groups by means of dynamic cell traction force microscopy (dCTFM). In this method, the iPS cell-derived cardiomyocytes will be seeded on top of a fibrinogen or collagen type I-coated polyacrylamide hydrogel with a Young's modulus of 10kPa. This hydrogel contains randomly located fluorescent microbeads which allowed visualising the hydrogel displacement upon cardiomyocyte contraction. Subsequently, vector displacement fields and total force developments will be calculated as described by Jacot et al. 2008[36] and Jacot et al. 2010.[33]. In order to approximate an *in vivo* setting, cardiomyocytes will be electrically stimulated. Pathway inhibitors or stimulators will be applied in order to determine the effect of several pathways on the cMyBP-C protein function. Ideally, no differences are observed between non-transfected and transfected control cardiomyocytes.

# 5. References


1. Maron BJ. Hypertrophic Cardiomyopathy A Systematic Review. Clin Cardiol. 2002;287(10).

2. Afonso LC, Bernal J, Bax JJ, Abraham TP. Echocardiography in hypertrophic cardiomyopathy: the role of conventional and emerging technologies. JACC Cardiovasc Imaging [Internet]. American College of Cardiology Foundation; 2008 Nov [cited 2015 Feb 15];1(6):787–800. Available from: http://www.ncbi.nlm.nih.gov/pubmed/19356516

3. Sadayappan S, de Tombe PP. Cardiac myosin binding protein-c: redefining its structure and function. Biophys Rev. 2012;4(2):93–106.

4. Harris SP, Lyons RG, Bezold KL. In the Thick of It: HCM-Causing Mutations in Myosin Binding Proteins of the Thick Filament. Circ Res. 2011;108(6):751–64.

5. Moolman-Smook J, Flashman E, de Lange W, Li Z, Corfield V, Redwood C, et al. Identification of Novel Interactions Between Domains of Myosin Binding Protein-C That Are Modulated by Hypertrophic Cardiomyopathy Missense Mutations. Circ Res [Internet]. 2002 Sep 12 [cited 2015 Mar 3];91(8):704–11. Available from: http://circres.ahajournals.org/cgi/doi/10.1161/01.RES.0000036750.81083.83

6. Squire JM, Luther PK, Knupp C. Structural Evidence for the Interaction of C-protein (MyBP-C) with Actin and Sequence Identification of a Possible Actin-binding Domain. J Mol Biol [Internet]. 2003 Aug [cited 2015 Mar 3];331(3):713–24. Available from: http://linkinghub.elsevier.com/retrieve/pii/S0022283603007812

7. Harris SP, Bartley CR, Hacker TA, McDonald KS, Douglas PS, Greaser ML, et al. Hypertrophic Cardiomyopathy in Cardiac Myosin Binding Protein-C Knockout Mice. Circ Res [Internet]. 2002 Jan 31 [cited 2015 Mar 6];90(5):594–601. Available from: http://circres.ahajournals.org/cgi/doi/10.1161/01.RES.0000012222.70819.64

8. Korte FS, McDonald KS, Harris SP, Moss RL. Loaded shortening, power output, and rate of force redevelopment are increased with knockout of cardiac myosin binding protein-C. Circ Res [Internet]. 2003 Oct 17 [cited 2015 Mar 9];93(8):752–8. Available from: http://www.ncbi.nlm.nih.gov/pubmed/14500336

9. Witayavanitkul N, Ait Mou Y, Kuster DWD, Khairallah RJ, Sarkey J, Govindan S, et al. Myocardial infarction-induced N-terminal fragment of cardiac myosin-binding protein C (cMyBP-C) impairs myofilament function in human myocardium. J Biol Chem [Internet]. 2014 Mar 28 [cited 2014 Nov 20];289(13):8818–27. Available from: http://www.pubmedcentral.nih.gov/articlerender.fcgi?artid=3979389&tool=pmcentrez&rendertype=abstract

10. Sánchez-Danés A, Richaud-Patin Y, Carballo-Carbajal I, Jiménez-Delgado S, Caig C, Mora S, et al. Disease-specific phenotypes in dopamine neurons from human iPS-based models of genetic and sporadic Parkinson's disease. EMBO Mol Med [Internet]. 2012 May [cited 2014 Sep 22];4(5):380–95. Available from: http://www.pubmedcentral.nih.gov/articlerender.fcgi?artid=3403296&tool=pmcentrez&rendertype=abstract

11. Takahashi K, Yamanaka S. Induction of pluripotent stem cells from mouse embryonic and adult fibroblast cultures by defined factors. Cell [Internet]. 2006 Aug 25 [cited 2014 Jul 9];126(4):663–76. Available from: http://www.ncbi.nlm.nih.gov/pubmed/16904174

12. Fusaki N, Ban H, Nishiyama A, Saeki K, Hasegawa M. Efficient induction of transgene-free human pluripotent stem cells using a vector based on Sendai virus, an RNA virus that does not integrate into the host genome. Proc Japan Acad Ser B [Internet]. 2009 [cited 2014 Oct 20];85(8):348–62. Available from: http://joi.jlc.jst.go.jp/JST.JSTAGE/pjab/85.348?from=CrossRef

13. Grossman M. Certificate of Analysis. CytoTune- iPS Sendai Reprogramming Kit. 2013 p. 1–2.

14. Invitrogen. CytoTune ™ -iPS Reprogramming Kit Catalog numbers A13780-01, A13780-02. 2012.

15. Chambers I, Colby D, Robertson M, Nichols J, Lee S, Tweedie S, et al. Functional Expression Cloning of Nanog, a Pluripotency Sustaining Factor in Embryonic Stem Cells. Cell [Internet]. 2003 May;113(5):643–55. Available from: http://linkinghub.elsevier.com/retrieve/pii/S0092867403003921

16. Dani C, Chambers I, Johnstone S, Robertson M, Ebrahimi B, Saito M, et al. Paracrine induction of stem cell renewal by LIF-deficient cells: a new ES cell regulatory pathway. Dev Biol [Internet]. 1998 Nov 1;203(1):149–62. Available from: http://www.ncbi.nlm.nih.gov/pubmed/9806780

17. Lian X, Zhang J, Azarin SM, Zhu K, Hazeltine LB, Bao X, et al. Directed cardiomyocyte differentiation from human pluripotent stem cells by modulating Wnt/ß-catenin signaling under fully defined conditions. Nat Protoc. 2013;8(1):162–75.

18. Yang L, Soonpaa MH, Adler ED, Roepke TK, Kattman SJ, Kennedy M, et al. Human cardiovascular progenitor cells develop from a KDR+ embryonic-stem-cell-derived population. Nature [Internet]. 2008 May 22 [cited 2014 Dec 30];453(7194):524–8. Available from: http://www.ncbi.nlm.nih.gov/pubmed/18432194

19. Laflamme M a, Chen KY, Naumova A V, Muskheli V, Fugate J a, Dupras SK, et al. Cardiomyocytes derived from human embryonic stem cells in pro-survival factors enhance function of infarcted rat hearts. Nat Biotechnol [Internet]. 2007 Sep [cited 2015 Jan 7];25(9):1015–24. Available from: http://www.ncbi.nlm.nih.gov/pubmed/17721512

20. Ueno S, Weidinger G, Osugi T, Kohn AD, Golob JL, Pabon L, et al. Biphasic role for Wnt / ␣ -catenin signaling in cardiac specification in zebrafish and embryonic stem cells. PNAS. 2007;104(23):9685–90.

21. Naito AT, Shiojima I, Akazawa H, Hidaka K, Morisaki T, Kikuchi A, et al. Developmental stage-specific biphasic roles of Wnt / ␣ -catenin signaling in cardiomyogenesis and hematopoiesis. PNAS. 2006;103(52):19812–7.

22. Horvath P, Barrangou R. CRISPR/Cas, the Immune System of Bacteria and Archaea. Science (80- ) [Internet]. 2010 Jan 8 [cited 2014 Jul 11];327(5962):167–70. Available from: http://www.ncbi.nlm.nih.gov/pubmed/20056882

23. Ran FA, Hsu PD, Wright J, Agarwala V, Scott DA, Zhang F. Genome engineering using the CRISPR-Cas9 system. Nat Protoc. 2013;8(11):2281–308.

24. Hsu PD, Lander ES, Zhang F. Development and Applications of CRISPR-Cas9 for Genome Engineering. Cell [Internet]. Elsevier; 2014 Jun 5 [cited 2014 Jul 9];157(6):1262–78. Available from: http://www.ncbi.nlm.nih.gov/pubmed/24906146

25. Aasen T, Raya A, Barrero MJ, Garreta E, Consiglio A, Gonzalez F, et al. Efficient and rapid generation of induced pluripotent stem cells from human keratinocytes. Nat Biotechnol [Internet]. 2008 Nov [cited 2015 Mar 17];26(11):1276–84. Available from: http://www.ncbi.nlm.nih.gov/pubmed/18931654

26. Nishino K, Toyoda M, Yamazaki-Inoue M, Fukawatase Y, Chikazawa E, Sakaguchi H, et al. DNA Methylation Dynamics in Human Induced Pluripotent Stem Cells over Time. PLoS Genet [Internet]. 2011 May [cited 2015 May 21];7(5):e1002085. Available from: http://www.pubmedcentral.nih.gov/articlerender.fcgi?artid=3102737&tool=pmcentrez&rendertype=abstract

27. Ryan MD, King a. MQ, Thomas GP. Cleavage of foot-and-mouth disease virus polyprotein is mediated by residues located within a 19 amino acid sequence. J Gen Virol [Internet]. 1991 Nov 1;72(11):2727–32. Available from: http://vir.sgmjournals.org/cgi/doi/10.1099/0022-1317-72-11-2727

28. Kim JH, Lee S-R, Li L-H, Park H-J, Park J-H, Lee KY, et al. High cleavage efficiency of a 2A peptide derived from porcine teschovirus-1 in human cell lines, zebrafish and mice. PLoS One [Internet]. 2011 Jan [cited 2014 Jul 10];6(4):e18556. Available from: http://www.pubmedcentral.nih.gov/articlerender.fcgi?artid=3084703&tool=pmcentrez&rendertype=abstract

29. Wu SC, Zhang Y. Active DNA demethylation: many roads lead to Rome. Nat Rev Mol Cell Biol [Internet]. Nature Publishing Group; 2010 Sep [cited 2014 Jul 11];11(9):607–20. Available from: http://www.pubmedcentral.nih.gov/articlerender.fcgi?artid=3711520&tool=pmcentrez&rendertype=abstract

30. Masters BR. Paths to Förster's resonance energy transfer (FRET) theory. Eur Phys J H [Internet]. 2013 Dec 23 [cited 2015 Mar 2];39(1):87–139. Available from: http://link.springer.com/10.1140/epjh/e2013-40007-9

31. Scholes GD. Long-range resonance energy transfer in molecular systems. Annu Rev Phys Chem [Internet]. 2003 Jan [cited 2014 Jul 14];54(18):57–87. Available from: http://www.ncbi.nlm.nih.gov/pubmed/12471171

32. Peter M, Ameer-Beg SM, Hughes MKY, Keppler MD, Prag S, Marsh M, et al. Multiphoton-FLIM quantification of the EGFP-mRFP1 FRET pair for localization of membrane receptor-kinase interactions. Biophys J [Internet]. Elsevier; 2005 Feb [cited 2015 Mar 22];88(2):1224–37. Available from: http://www.pubmedcentral.nih.gov/articlerender.fcgi?artid=1305125&tool=pmcentrez&rendertype=abstract

33. Jacot JG, Kita-Matsuo H, Wei K a, Chen HSV, Omens JH, Mercola M, et al. Cardiac myocyte force development during differentiation and maturation. Ann N Y Acad Sci [Internet]. 2010 Feb [cited 2014 Dec 4];1188(Analysis of Cardiac Development):121–7. Available from: http://www.pubmedcentral.nih.gov/articlerender.fcgi?artid=2920416&tool=pmcentrez&rendertype=abstract

34. Wozniak M a, Modzelewska K, Kwong L, Keely PJ. Focal adhesion regulation of cell behavior. Biochim Biophys Acta [Internet]. 2004 Jul 5 [cited 2015 Feb 19];1692(2-3):103–19. Available from: http://www.ncbi.nlm.nih.gov/pubmed/15246682

35. Meikle MC. The tissue, cellular, and molecular regulation of orthodontic tooth movement: 100 years after Carl Sandstedt. Eur J Orthod [Internet]. 2006 Jun [cited 2015 Mar 23];28(3):221–40. Available from: http://www.ncbi.nlm.nih.gov/pubmed/16687469

36. Jacot JG, McCulloch AD, Omens JH. Substrate stiffness affects the functional maturation of neonatal rat ventricular myocytes. Biophys J [Internet]. 2008 Oct [cited 2015 Feb 19];95(7):3479–87. Available from: http://www.pubmedcentral.nih.gov/articlerender.fcgi?artid=2547444&tool=pmcentrez&rendertype=abstract

37. Oakley CE, Hambly BD, Curmi PMG, Brown LJ. Myosin binding protein C : Structural abnormalities in familial hypertrophic cardiomyopathy. Cell Res. 2004;14(2):95–110.

38. Cong L, Ran FA, Cox D, Lin S, Barretto R, Habib N, et al. Multiplex Genome Engineering Using CRISPR/Cas Systems. Science [Internet]. 2012 Feb 15 [cited 2014 Jul 9];339(6121):819–23. Available from: http://www.pubmedcentral.nih.gov/articlerender.fcgi?artid=3795411&tool=pmcentrez&rendertype=abstract

39. Inestrosa NC, Varela-nallar L. Chapter 4: Wnt Signaling Roles on the Structure and Function of the Central Synapses : Involvement in Alzheimer ' s Disease. Trends in Cell Signaling Pathways in Neuronal Fate Decision. 2013. p. 115–40.

# 6. Appendix

## Supplemental figures

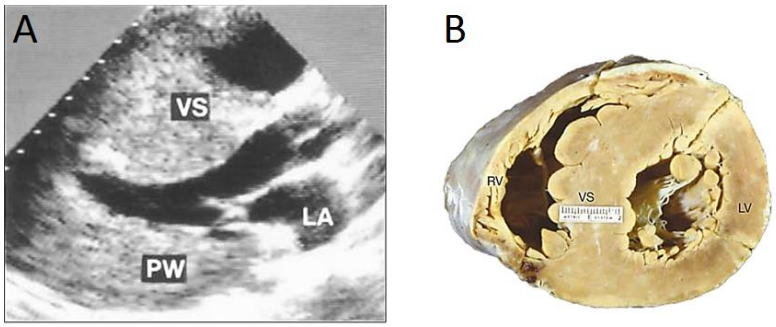


**SUPPLEMENTAL FIGURE S1 Hypertrophic cardiomyopathy.** ***Panel A Echocardiogram of a heart with hypertrophic cardiomyopathy*** [1]**.** In this case severe hypertrophia was observed in the ventricular septum (VS) and the posterior wall (PW). (LA=left atrium). ***Panel B Cross-section of a heart with hypertrophic cardiomyopathy from a basal viewpoint*** [1]. A clear hypertrophia is visible at the level of the ventricular septum (VS) and the posterior wall of the left ventricle (LV). (RV=Right ventricle).

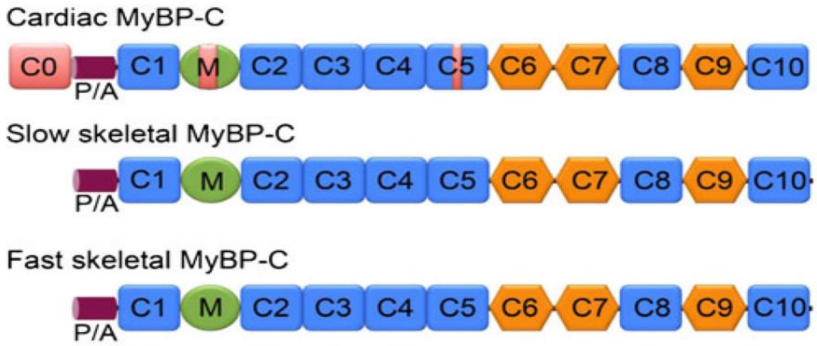


**SUPPLEMENTAL FIGURE S2 Structure of MyBP-C family members** All MyBP-C isoforms displayed have 7 immunoglobulin domains and 3 fibronectin type III domains in common. However, cMyBP-C differs from the skeletal isoforms in the presence of an additional N-terminal C0 immunoglobulin domain, multiple phosphorylation sites in the M-domain and an additional 28 amino acid residues in the C5 domain [3].

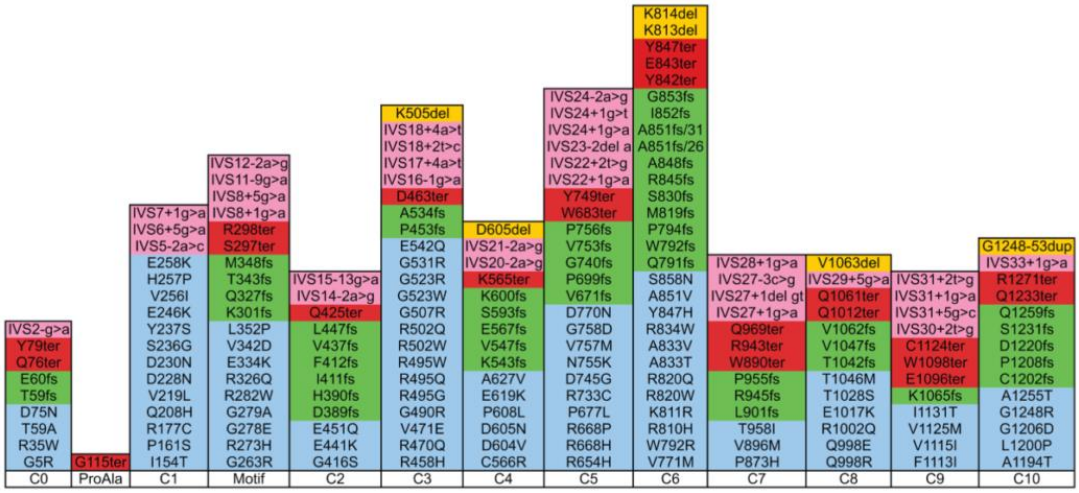


**SUPPLEMENTAL FIGURE S3 All 197 known cMyBP-C mutations** [**4**] Mutations are given for each domain of cMyBP-C. A large part of the mutations are missense mutations leading to single amino acid substitutions that do not alter the rest of the protein (Blue). Other mutations have been identified as frameshift mutations, who thus lead to truncated and non-functional proteins (Green). A third group are those mutations that lead to a premature stop codon which leads to the production of truncated proteins (Red). Even more, there are splice donor and acceptor mutations which lead to splicing deviations of the mRNA transcript (Pink). Lastly, six insertion or deletion mutations (Yellow) have been identified that do not alter the open reading frame.

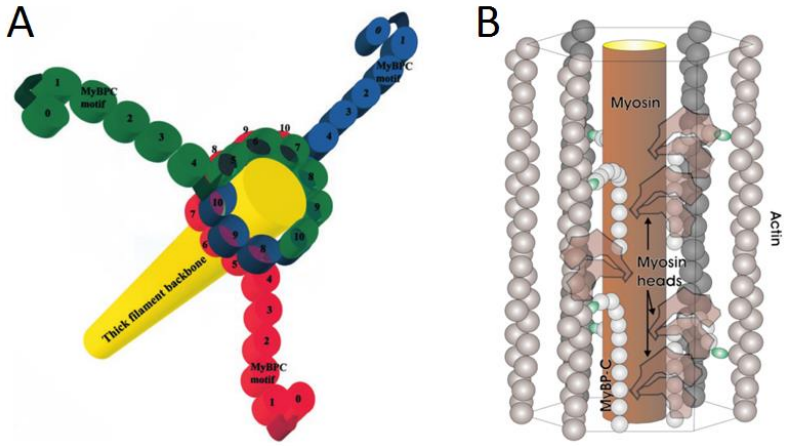


**SUPPLEMENTAL FIGURE S4 Proposed models for cMyBP-C position and alignment.** ***Panel A Trimeric collar model*** This model proposes a trimerisation of cMyBP-C with a collar-like orientation around the myosin filament. Release of strain on the thick filament by this collar would facilitate myosin head movement and hence accelerate cross-bridge cycling. Evidence for C5:C8 interaction supports this model [5]. ***Panel B Rod model of axial arrangement*** This model shows a parallel alignment of the C-terminal part of cMyBP-C with the myosin thick filament [6].

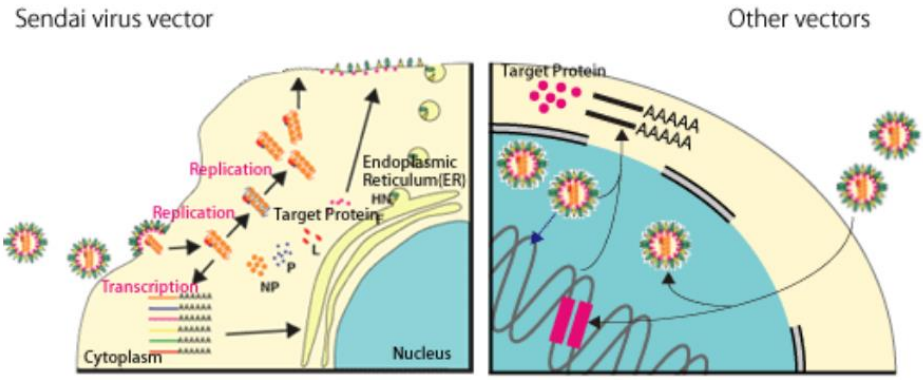


**SUPPLEMENTAL FIGURE S5 Transduction with Sendai virus vectors and other vectors** [14] Sendai virus vectors do not integrate into the target cell's genome and therefore do not induce genomic alterations and subsequent carcinogenicity. Vector proteins are expressed in the target cell's cytoplasm without any vector entering the nucleus. In contrast, other vectors, such as retroviruses, randomly insert their DNA sequences into the target cell's genome. Consequently, not only is the vector protein expression in this case dependent on the endogenous governing promotor but may also induce carcinogenicity or toxicogenicity by disruption of endogenous genes.

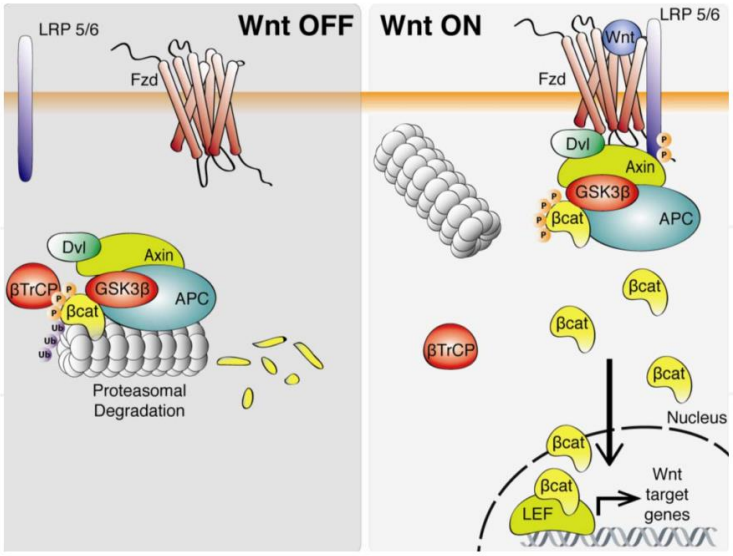


**SUPPLEMENTAL FIGURE S6 Wnt Pathway** [39] ***Left panel Wnt*** OFF In the absence of stimulation by Wnt, a multiprotein complex containing GSK3ß phosphorylates ß-catenin and targets it for ubiquitin proteasome degradation. ***Right panel Wnt ON*** In case of Wnt ligand binding to Fzd and LRP5/6 receptors, the multiprotein complex associates with these receptors and GSK3ß still phosphorylates ß-catenin but does not target it any longer for ubiquitin proteasome degradation. ß-catenin then functions as gene expression activator.

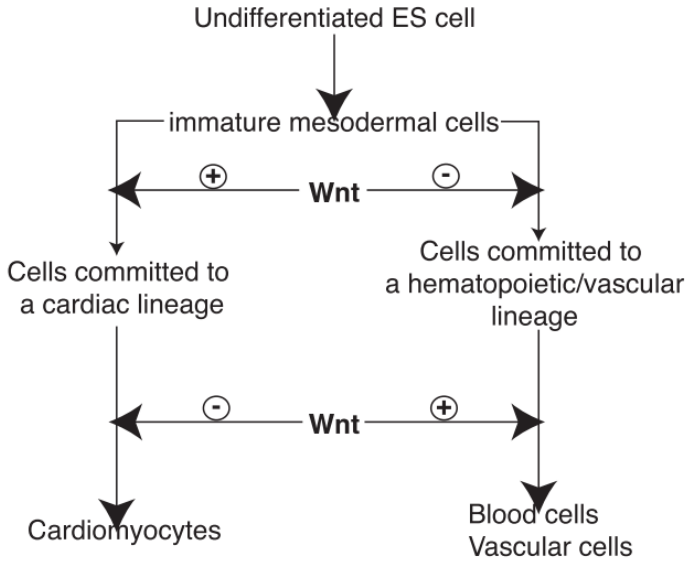


**SUPPLEMENTAL FIGURE S7** [21] **Effects of Wnt pathway signalling on ES cell lineage commitment** Early Wnt pathway signalling has been shown to promote cardiogenesis but inhibit haematopoiesis in an early stage of differentiating ES cells. In contrast, in a later stage of differentiation, Wnt pathway signalling negatively affects cardiogenesis while stimulating haematopoiesis.

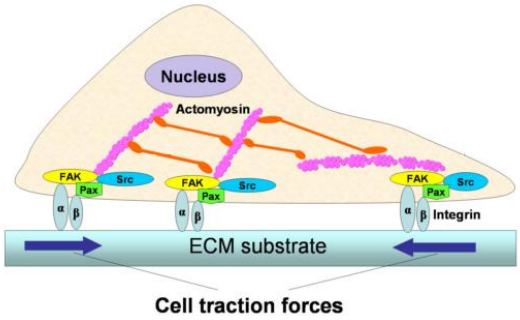


**SUPPLEMENTAL FIGURE S8 Cell traction force generation**. Cells generate force by sensing the substrate by means of focal adhesions. Focal adhesions include integrins, FAK , paxillins and Src. These proteins transmit substrate features such as the stiffness to the inner cell actomyosin network which in turn responds by generating forces.

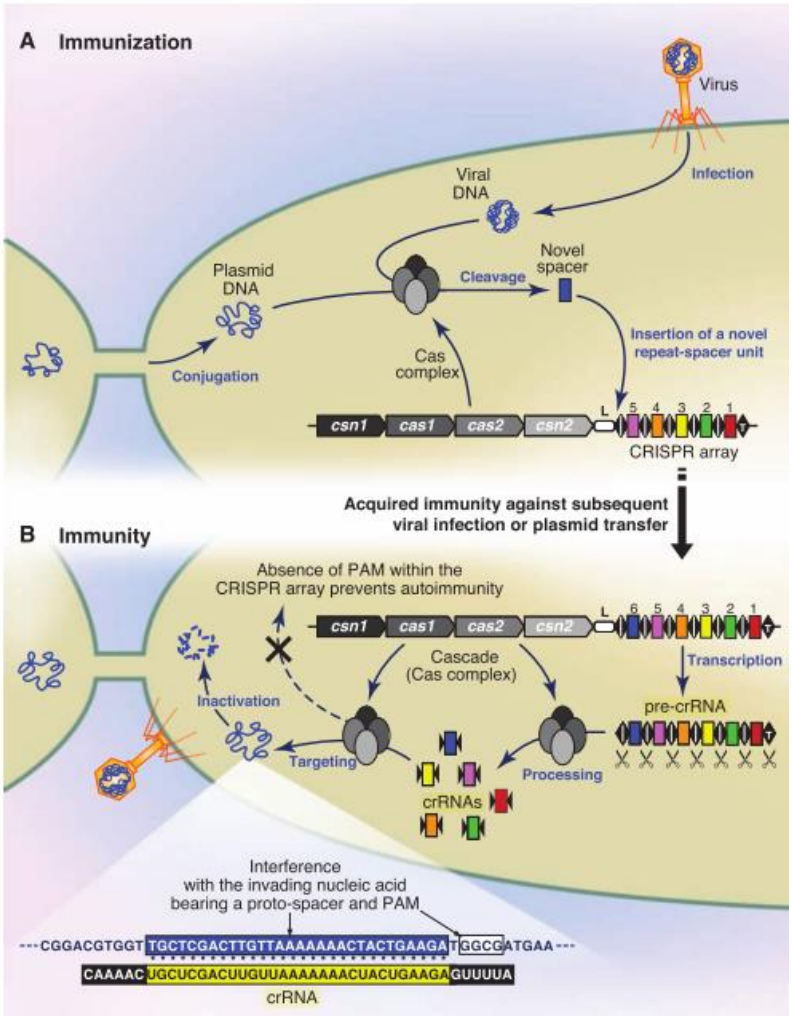


**SUPPLEMENTAL FIGURE S9 Bacterial CRISPR-Cas9 defence mechanism** [22]**.** The CRISPR-Cas9 system is a defence mechanism of many bacteria. **A. Immunisation**. Upon a first viral infection of a bacterium, the Cas complex cleaves the viral DNA into a new spacer to be integrated into the CRISPR region. **B. Immunity**. The new spacer in the CRISPR region gives rise to a crRNA which guides the Cas complex to a specific target sequence in the viral DNA. The Cas complex then cleaves and inactivates the viral DNA, hence inducing immunity for this virus.

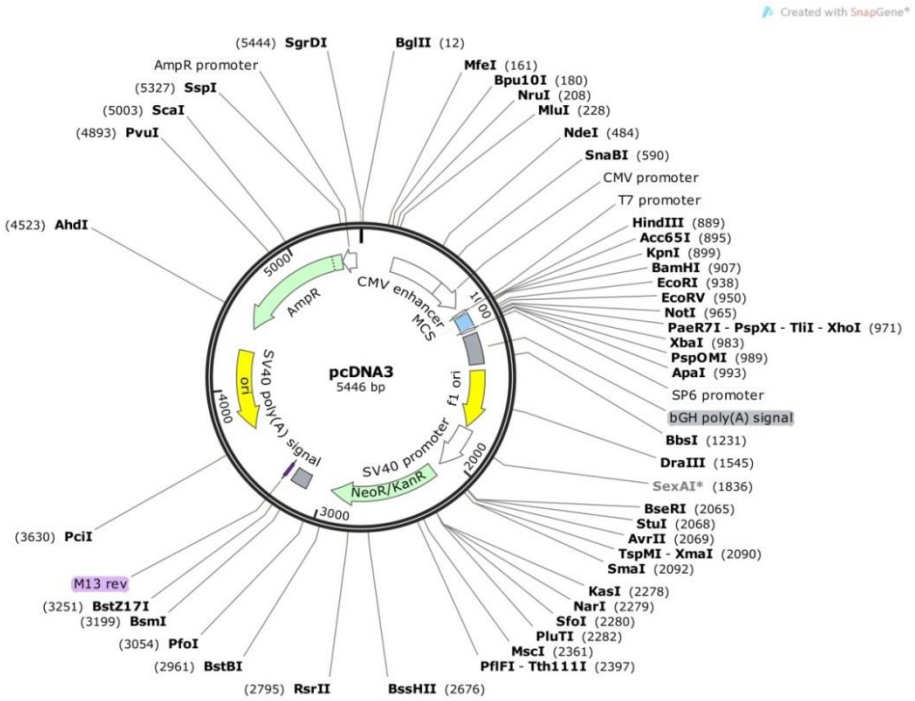


**SUPPLEMENTAL FIGURE S10 pcDNA3 vector with the original neomycin resistance cassette.**

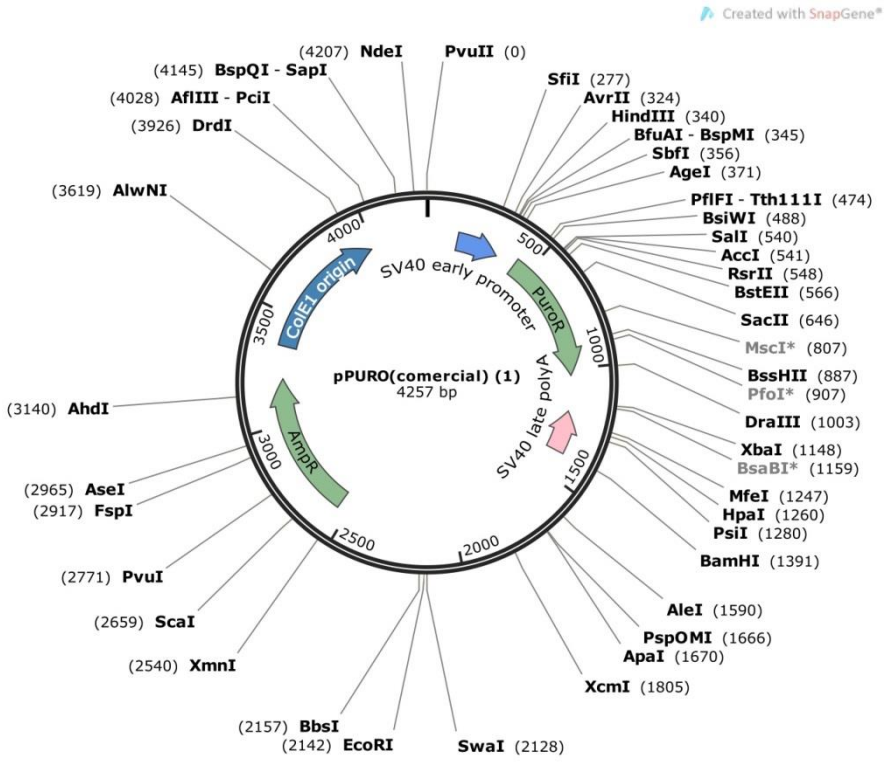


**SUPPLEMENTAL FIGURE S11 pPuro vector containing the puromycin resistance cassette.**

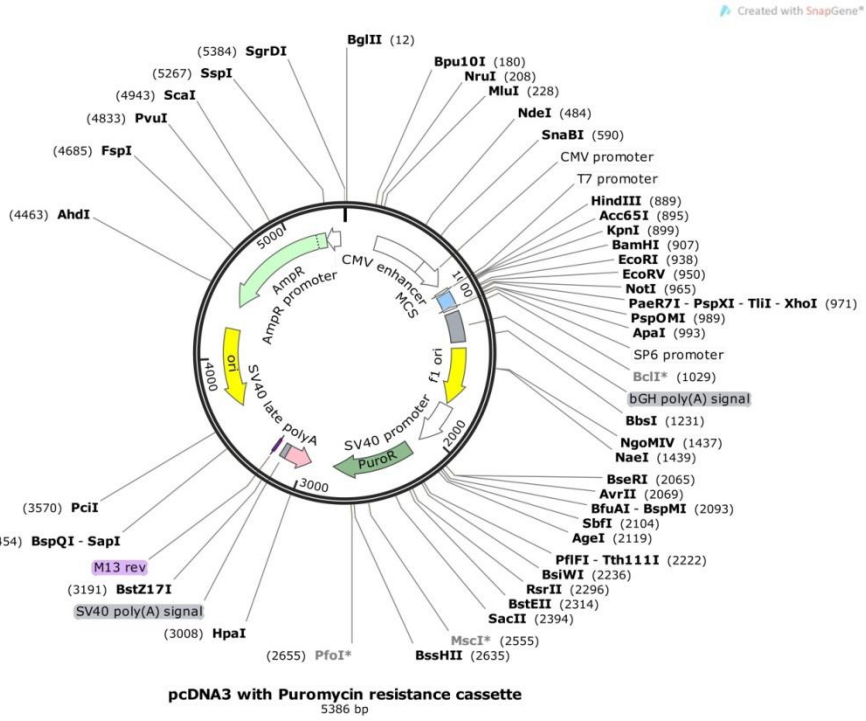


**SUPPLEMENTAL FIGURE S12 pcDNA3 vector with the puromycin resistance cassette.**

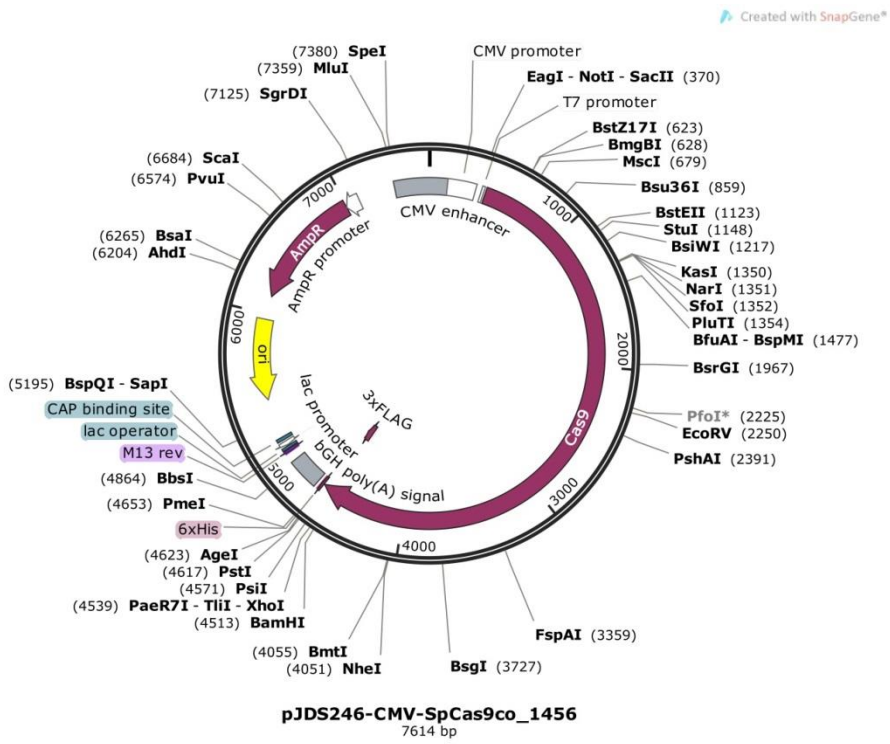


**SUPPLEMENTAL FIGURE S13 pMLM3705 vector encoding Cas9**

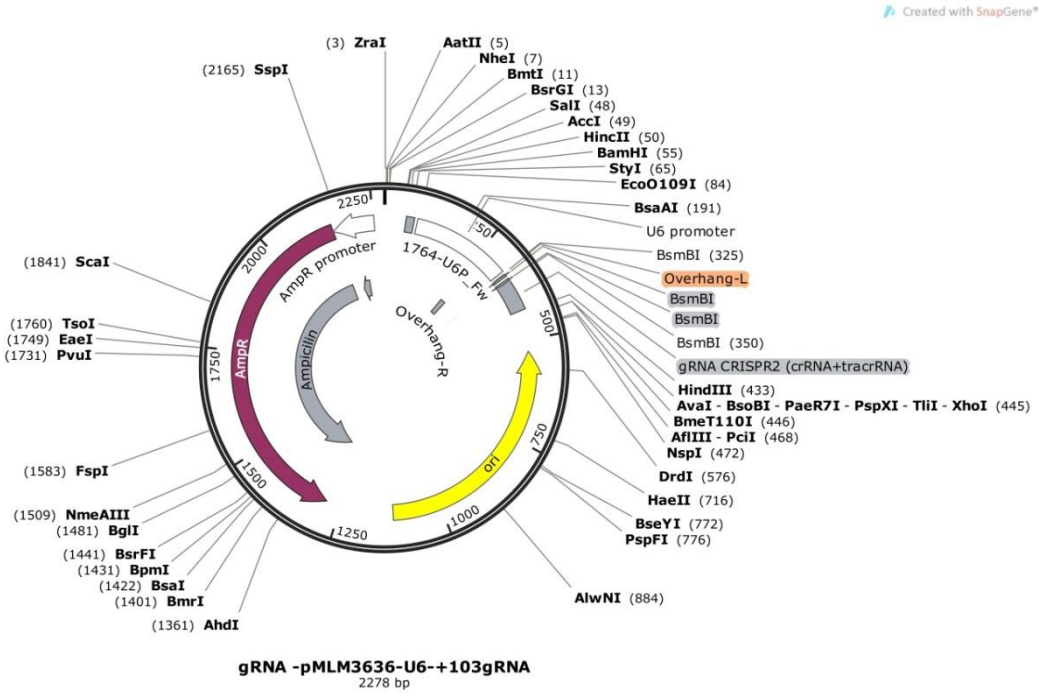


**SUPPLEMENTAL FIGURE 14 pMLM3636 vector encoding the gRNA oligosequences together with the tracrRNA**

# Auteursrechtelijke overeenkomst

Ik/wij verlenen het wereldwijde auteursrecht voor de ingediende eindverhandeling:
**Assessing actin-cMyBP-C interactions in IPS cell-derived cardiomyocytes**

Richting: **master in de biomedische wetenschappen-klinische moleculaire wetenschappen**
Jaar: **2015**

in alle mogelijke mediaformaten, - bestaande en in de toekomst te ontwikkelen - , aan de Universiteit Hasselt.

Niet tegenstaand deze toekenning van het auteursrecht aan de Universiteit Hasselt behoud ik als auteur het recht om de eindverhandeling, - in zijn geheel of gedeeltelijk -, vrij te reproduceren, (her)publiceren of distribueren zonder de toelating te moeten verkrijgen van de Universiteit Hasselt.

Ik bevestig dat de eindverhandeling mijn origineel werk is, en dat ik het recht heb om de rechten te verlenen die in deze overeenkomst worden beschreven. Ik verklaar tevens dat de eindverhandeling, naar mijn weten, het auteursrecht van anderen niet overtreedt.

Ik verklaar tevens dat ik voor het materiaal in de eindverhandeling dat beschermd wordt door het auteursrecht, de nodige toelatingen heb verkregen zodat ik deze ook aan de Universiteit Hasselt kan overdragen en dat dit duidelijk in de tekst en inhoud van de eindverhandeling werd genotificeerd.

Universiteit Hasselt zal mij als auteur(s) van de eindverhandeling identificeren en zal geen wijzigingen aanbrengen aan de eindverhandeling, uitgezonderd deze toegelaten door deze overeenkomst.

Voor akkoord,

**De Smedt, Jonathan**

Datum: **9/06/2015**